ORIGINAL PAPER

Comparative vegetation survey with focus on cryptogamic covers in the high Arctic along two differing catenas

Ramona Kern[1], Vivien Hotter[1], Aline Frossard[2], Martin Albrecht[1], Christel Baum[6], Bjorn Tytgat[3], Lotte De Maeyer[3], David Velazquez[4], Christophe Seppey[5], Beat Frey[2], Michael Plötze[7], Elie Verleyen[3], Antonio Quesada[4], Mette M. Svenning[5], Karin Glaser[1], Ulf Karsten[1*]

[1]University of Rostock, Institute of Biological Sciences, Applied Ecology and Phycology, D-18059 Rostock, Germany

[2] Swiss Federal Research Institute WSL, CH-8903 Birmensdorf, Switzerland

[3]Ghent University, Department of Biology, Protistology and Aquatic Ecology, B-9000 Gent, Belgium

[4]Universidad Autónoma de Madrid, Department of Biology, E-28049 Madrid, Spain

[5]UiT The Arctic University of Norway, Department of Arctic and Marine Biology, Faculty of Biosciences, Fisheries and Economics, N-9037 Tromsø, Norway.

[6]University of Rostock, Soil Sciences, Faculty of Agricultural and Environmental Sciences, D-18059 Rostock, Germany

[7]ETH Zurich, Institute for Geotechnical Engineering, ClayLab, CH-8093 Zürich, Switzerland

***Correspondence:**

Corresponding Author

Prof. Dr. Ulf Karsten, email: ulf.karsten@uni-rostock.de

Keywords

Arctic, Svalbard, cryptogamic cover, soil, moisture, tundra, vegetation survey

Abstract

Although cryptogamic covers are important ecosystem engineers in high Arctic tundra, they were often neglected in vegetation surveys. Hence we conducted a systematic survey of cryptogamic cover and vascular plant coverage and composition at two representative, but differing Arctic sites (Ny-Ålesund, Svalbard) along catenas with a natural soil moisture

gradient, and integrated these data with physical-chemical soil properties. Soil samples were taken for comprehensive pedological and mineralogical analyses. Vegetation surveys were conducted based on classification by functional groups. Vascular plants were identified to species level. Correlation and multivariate statistical analysis were applied to determine the key environmental factors explaining vegetation patterns along the soil moisture gradients. We observed significant differences in gravimetric water, soil organic matter and nutrient contents along the moisture gradients. These differences were coincident with a shift in vegetation cover and species composition. While chloro- and cyanolichens were abundant at the drier sites, mosses dominated the wetter and vascular plants the intermediate plots. Twenty four vascular plant species could be identified, of which only six were present at both sites. Cryptogamic covers generally dominated with maximum areal coverage up to 70% and hence should be considered as a new additional syntaxon in future ground-truth and remote sensing based vegetation surveys of Svalbard. Multivariate analysis revealed that soil moisture showed the strongest relation between vegetation patterns, together with NH_4-N and pH. In conclusion, soil moisture is a key driver in controlling cryptogamic cover and vegetation coverage and vascular plant species composition in high Arctic tundra.

Introduction

Cryptogamic covers are, together with dwarf shrubs, forbs and graminoids, the dominant primary producers in High Arctic tundra biomes (Breen and Levesque 2006; Williams et al. 2017). Cryptogamic covers consist of different functional community types such as biological soil crusts (biocrusts) that are generally considered as an early successional stage dominated by various microorganisms such as algae and protists, as well as bacteria, archaea and fungi (Elbert et al. 2012). Later successional stages of cryptogamic covers are dominated by lichens and mosses, respectively, depending on the water availability (Elbert et al. 2012). Cryptogamic covers reach an average areal coverage of 50 %, with a high local variability ranging from 18 up to even 90 %, making them the dominant vegetation type at many High Arctic locations (Pushkareva et al. 2016; Williams et al. 2017). Despite this, cryptogamic covers are often neglected in ground-based vegetation surveys and large-scale vegetation mapping using satellite imagery of Svalbard and other Arctic regions (Johansen et al. 2012; Johansen and Tømmervik 2014).

Cryptogamic covers are formed by living organisms and their by-products, creating a few millimeters to centimeter thick top-soil layer of inorganic particles bound together by organic materials. They are often regarded as ‘ecosystem-engineers’, as they form water-stable

aggregates that have important, multi-functional ecological roles in primary production, nutrient and hydrological cycling, mineralization, weathering, and the stabilization of soils (Castillo-Monroy et al. 2010). More in particular, on a global scale, cryptogamic covers significantly contribute to C fixation (about 7 % of the total terrestrial vegetation) and N fixation (about 50 % of the total terrestrial biological N fixation) (Elbert et al. 2012). Since both cyanobacteria and algae excrete extracellular polymeric substances (EPS) which glue soil particles together, they form a carpet-like crust that increases the resistance against soil erosion by wind and water. By capturing water, cryptogamic covers also control the moisture content and buffering capacity of soils against temperature fluctuations. As such, cryptogamic covers s influence soil processes, thereby facilitating the colonization of previous barren substrates by vascular plants (Pushkareva et al. 2016; Williams et al. 2017). Cryptogamic covers are therefore regarded as an important component in 'the greening of the Arctic'(Screen and Simmonds 2010).

In the Arctic, water availability depending on habitat (micro)topography is, as elsewhere, a key driver in controlling the vegetation density and species composition (Zhang et al. 2004). An illustration of representative Arctic vegetation toposequences are given in Figure 7. Elevated ridges are generally exposed to wind, so that snow is easily blown away, leaving behind only a thin snow layer as source of melt water, in turn leading to rather dry ridge soils. The slopes directly beneath these ridges benefit from meltwater runoff and thus represent mesic sites. As the snow gets blown away, it accumulates in snow beds below the exposed ridges. In spring and summer, melting of these snow banks results in a soil moisture gradient that increases downhill. Eventually, excessive meltwater gathers in depressions, supplying wetlands, lakes and ponds (Elvebakk 1994; Walker 2000). This moisture gradient is reflected in the dominant vegetation types in Arctic tundra biomes. Dry exposed ridges are covered with open vegetation mainly consisting of prostrate dwarf-shrubs such as *Dryas octopetala* and lichenized biocrusts. In more moist habitats, prostrate dwarf-shrubs like *Salix polaris* and scattered herbs like *Saxifraga oppositifolia* and *Oxyria digyna* are the dominant vascular plants. In between these vascular plants cryptogamic covers can reach a surface coverage of up to 63% (e.g. station Brandal, Williams et al. 2017). Towards the wettest sites, pleurocarp mosses (and hence moss dominated cryptogamic covers) take over along with grasses and sedges (Elvebakk 1999). In addition, Pushkareva et al. (2015) reported that the soil water content shaped the cyanobacterial community composition of Arctic biocrusts. The increase of soil water content resulted in higher cyanobacterial richness.

Not only is the gradient in vegetation functional types directly influenced by the nutrient and organic carbon concentrations of the underlying soils, the vegetation itself also exerts a strong control on the remineralization of organic matter by microorganisms present (Berg and Smalla 2009; Vimal et al. 2017). In general, wet tundra is characterized by higher N and C contents compared to dry systems, but the available information is contradictory between studies, probably as a result of patchiness in vegetation types and soil properties (Chapin III and Shaver 1981; Edwards and Jefferies 2013).

We aimed to assess the relation between physico-chemical soil parameters along catenas on the composition and coverage of cryptogamic covers and vascular plants in the High Arctic tundra. Both catenas ranged from a wet site (wetland or close to a lake) to a hill or an elevated ridge, respectively, at two sampling sites (Knudsenheia (KH) and Ossian-Sarsfjellet (OS)) (see also Fig. 7). Both sites represent typical settings in the High Artic: one is a coastal plain with a soft slope towards a wetland (KH), the other an elevated ridge with a steep slope towards a permanent lake (OS). We assumed that soil moisture is one of the key factors influencing the vegetation type. As the water availability influences and is influenced by various soil parameters and vegetation, we conducted in-depth analyses of various pedological parameters as well as vegetation surveys including cryptogamic covers and vascular plants.

Materials and Methods

Study sites

The Ny-Ålesund Research Station (Svalbard, Norway, 78°55′26.33’’N, 11°55′23.84’’E), with contributions from many institutions and countries, is a model system for the High Arctic. Ny-Ålesund represents a coastal terrestrial environment, which is characterized by a variety of different geological features, soil and glacier types, and hence habitats such as polar semi-desert, wet moss tundra, and ornithogenic soils. Because of the West Spitsbergen Current, which flows along the West coast of Svalbard and transports warm Atlantic water masses into the Arctic Ocean, Ny-Ålesund shows relatively mild climatic conditions compared to other regions at the same latitude. A weather station was established in July 1974 by the Norwegian Meteorological Institute (www.met.no), which is located 8 m a.s.l., 100 m away from Ny-Ålesund. The meteorological data over the last two decades show a mean summer and winter temperature of 8 °C and -14 °C, respectively. However, longer cold periods between -20 °C and -35 °C can occur during winter. The annual precipitation over the last two decades averages 470 mm with 70 % typically falling between October and May, when snow cover is

usually complete, while the other 30 % are typically represented by scattered rain. Two sites were selected in the study area and established as permanent sampling sites, namely (1) Knudsenheia (KH), a wetland located approximately three km north-east of Ny-Ålesund, and (2) Ossian-Sarsfjellet (OS), a Nature Reserve approximately 12 km north-west of Ny-Ålesund across Kongsfjorden (Figs 1, 2). At each site a catena was established, which represent two different common settings in High Arctic tundra. KH is a typical coastal plain with a wetland at the flattest point (26 – 36 m a.sl.). In contrast, the catena in OS ranges from a permanent lake to an elevated ridge (100 – 113 m a.s.l.), a typical setting for inland areas (Fig. 1). More details on cryptogamic cover vegetation types along changing altitudes in Svalbard are given by Williams et al. (2017).

Experimental design and sampling

The catena in KH starts from the north to north-eastern littoral zone of a shallow pond and runs towards the south-southwest along a gradient in decreasing soil moisture (Figs 1C, 7). In OS, the wet plots are situated on the north to north-western shore of the lake Sarsvatnet. The catena was installed along a north by western orientation and culminates in a dry exposed ridge (Fig. 1D, 7).

Along each catena, three sub-sites were selected, namely dry, intermediate and wet. In each sub-site, three permanent replicate plots of 1 m² square were established (3 x 3 replicate plots per catena) (Table 1). Each 1 m² plot was further divided into four quadrats (50 x 50 cm) of which three were randomly used for soil sampling. Two different soil depths were consequently sampled with a sterilized spoon: the top layer (0-1 cm) and the subsoil (5-10 cm). In total, 54 soil samples (3 sub-sites differing in soil moisture content x 3 plots (replicates) x 3 quadrats x 2 soil depths) were collected per site. Each soil sample was filled into sterile plastic bags wherein the samples were homogenized by hand. Subsamples of these pooled samples were dried at 60 °C within 24 h after collection for subsequent soil analyses. The sampling campaign took place in summer 2017.

Pedological characterisation

Directly next to each dry, intermediate and wet plot a soil profile was excavated (about 1 m distance to the respective plots) as a rectangular pit down to 40 cm depth. Particularly the thickness of the O and A horizons was visually inspected based on characteristic colour changes and measured using a ruler. Soils were classified according to IUSS Working Group WRB (2015) protocol (The International Union of Soil Sciences, https://www.iuss.org).

For water content determination of each sample, about 20 g of fresh soil from one of the 50 x 50 cm quadrats were sieved (2 mm mesh) and weighed. Afterwards, the soil was dried at 105 °C overnight. After weighing again, the gravimetric soil water content was calculated. This dried soil fraction was subsequently combusted at 450 °C for 5 h for the assessment of the amount of the soil organic matter content. The moisture content was expressed as percentage of total fresh mass and the organic matter content percentage of total dry mass.

The pH of each soil sample was measured in an aqueous soil-extract (soil:aqua ratio of 1:2) with a glass electrode connected to a pH meter (FEP20-FiveEasy Plus, Mettler-Toledo GmbH, Switzerland).

Soil texture (percentage of sand, silt, clay) of each soil sample was determined following the „sieve-pipette“ approach (Gee and Bauder 1986). This method is a combination of wet sieving of the fraction >63 µm and the pipette sampling method for the silt (2–63 µm) and clay (<2 µm) fractions. In a column, the sediment concentration, as a function of time, was monitored by timed withdrawals of samples with a pipette at certain heights and at a constant temperature. The sieve-pipette method measures the mass percentage for the defined grain-size classes.

For nutrient analysis, dried soil subsamples (see above) were sieved (2 mm mesh). These subsamples were stored at room temperature prior to further analysis. For ammonia and nitrate analysis 0.5 g of dried and ground soil was extracted with 20 mL of 0.01 mol L^{-1} $CaCl_2$ for 2 h on a vertical shaker. Afterwards, each extract was filtered with a GF92 glass-fiber filter (Whatman) and the filtrate was frozen at -20 °C until measurement with a continuous flow analyser (Alliance Instruments, Salzburg, Austria) using the manufacturer’s protocol for both compounds. Two soluble labile inorganic phosphate fractions according to Hedley et al. (1982) were extracted by a two-step fractionation scheme, the first consisting of the water-extract and the second one of the bicarbonate-extract. Five grams of pooled dried and ground soil samples were transferred into 20 mL of ultra-pure de-ionized water and incubated on a vertical shaker for 24 h. The tubes were then centrifuged for 5 min at 5,000 rpm (Megafuge, Heraeus) and the supernatant was filtrated with glass-fiber filters (MN 616 G - phosphate-free), resulting in the water-extract. The soil-pellet was re-suspended in 20 mL 0.5 mol L^{-1} $NaHCO_3$ solution and put again onto a vertical shaker for 24 h, followed by centrifugation and filtration as in the first extraction step. The bicarbonate-filtrate was neutralized (pH 7) prior to measurement. The filtrates and neutralized filtrates were then measured for their P concentrations using the colorimetrical molybdenum blue method at λ = 885 nm (Murphy and Riley 1962). The soil total carbon (TC) and total nitrogen (TN) were determined from these

dried and ground soil subsamples by dry combustion using a CNS VARIO EL analyser (Elementar Analysensysteme GmbH, Germany).

Mineralogy of bulk samples was determined on randomly oriented powder specimens with X-ray diffraction (XRD) analysis. The samples were air dried, crushed in a jaw breaker <400 µm and split representatively. An aliquot of about 2 g was milled in ethanol to a grain size below 20 µm with a McCrone micronizing mill and dried afterwards at 65 °C. For frontloading preparation, about 1 g of the powdered material was gently pressed in a sample holder for packing, sample-height adjustment and forming a flat surface. Preferred orientation was avoided by using a blade for surface treatment. A second sample preparation was carried out producing oriented specimens for enhancement of the basal reflexes of layer silicates, thereby facilitating their identification. The changes in the reflex positions in the XRD pattern by intercalation of different organic compounds (e.g. ethylene glycol) and after heating were used for identification in particular of smectite.

X-ray diffraction measurements were conducted with a Bragg-Brentano X-ray diffractometer (D8 Advance, Bruker AXS, Germany) using CoKα (35 kV, 40 mA) radiation. The instrument was equipped with an automatic theta compensating divergence slit and a Lynx-Eye XE-T detector. The powder samples were step-scanned at room temperature from 2 to 80°2Theta (step width 0.02°2Theta, counting time 2 s per step). The qualitative phase analysis was carried out with the software package DIFFRACplus (Bruker AXS). The phases were identified on the basis of the peak positions and relative intensities in the comparison to the PDF-2 data base (International Centre for Diffraction Data).

The quantitative amount of the mineral phases was determined with Rietveld-analysis. This full pattern-fitting method consists in the calculation of the X-ray diffraction pattern and its iterative adjustment to the measured diffractogram. In the refinements phase specific parameters and the phase content were adapted to minimize the difference between the calculated and the measured X-ray diffractogram. The quantitative phase analysis was carried out with Rietveld program Profex/BGMN (Döbelin and Kleeberg 2015).

Vegetation survey

All vegetation surveys were carried out, together with the soil sampling, in late July and early August 2017. At both field sites, each of the 18 permanent sampling plots was evaluated by manual inspection and documentation using a digital camera (see Online Resource 1 and 2). Additionally, three vegetation survey plots of 25 x 25 m were established along the soil moisture gradient in both field sites. The vegetation of these plots was recorded following the

point intercept method (Levy and Madden 1933) to determine the proportions of eight ground cover functional groups according to the approach of Williams et al. (2017). These included biocrusts (typically dominated by cyanobacteria, which cause a dark color), chlorolichen (with an algal photobiont), cyanolichen (with a cyanobacterial photobiont), moss, vascular plant, litter (dead plant material, reindeer and goose droppings), rock, and bare soil. Litter, rock, and bare soil were later on summarized as 'unvegetated area'. Twenty-five squares of 25 x 25 cm (=625 cm^2) were randomly selected within each established vegetation survey plot, and the functional groups in each square were determined by 25 point measurements (Levy and Madden 1933). In total, 625 point measurements per vegetation survey plot were undertaken. The vascular plant species on the vegetation survey and the experimental plots were determined after Rønning (1996), and the names corrected according to the Plant List 2013 (www.theplantlist.org).

Statistical analyses

All statistical analyses were done using R version 3.4.0 (R-Development-Core-Team 2017). The mean of the replicate quadrants (see above) was calculated and used for further statistical analysis. After a Shapiro-Wilk test for normality, analysis of Variance (one-way ANOVA) was performed to reveal significant differences of the measured soil parameters between the subsites (wet, intermediate, dry) in both regions, with a threshold of significance at 95 %. The soil parameters were normalized ($X_{norm}=(X_i-X_{min})/(X_{max}-X_{min})$) for cluster and multivariate analyses. A cluster analysis based on the Bray-Curtis dissimilarity was conducted to visualize differences within and between the sites according to the measured soil parameters using the Vegan package (Oksanen et al. 2018) implemented in R.

With the data obtained via the point intercept method, the percentage areal coverage by each functional group was calculated for every plot and displayed in a stacked bar plot. Moreover, differences in vegetation coverage between the plots were visualized by non-metric multidimensional scaling (nMDS) using the Vegan package and Bray-Curtis dissimilarity index implemented in R. To reveal correlations between the ground coverage of the vegetation classes and soil parameters, permutational multivariate analysis of variance (PERMANOVA) (with the "adonis" function in R) was applied using the Bray–Curtis dissimilarity index, including a permutation test with 1000 permutations. Soil parameters that were significantly correlated with vegetation ground cover were added to the plot. Subsequently, the data on ground coverage were statistically analyzed via pairwise PERMANOVA implemented in the RVAideMemoire package (Hervé 2018) followed by

Bonferroni correction to compare the ground coverage composition along the transect and among the investigated sites. The presence/absence data of the vascular plants were visualized with a Venn diagram using the Venn diagram package (Dusa 2017) implemented in R.

Results

Physical and chemical soil properties

The cluster analysis based on all physical and chemical soil parameters (Table 1) revealed a clear separation between the KH and OS sites, as well as between the dry, intermediate and wet plots in both regions (Fig. 3). One exception is KHd.1 which clustered separately from the other dry KH plots, because of its much lower moisture content (14.7 % compared to 35.8 and 33.4 %, respectively). Especially for OS, the cluster analyses revealed a clear difference between each subsite (dry, intermediate and wet) but a close similarity between the replicate plots. The differences between the subsites are also reflected in the mean values of the physical and chemical soil parameters (Table 1).

The different KH plots were characterized by higher sand (75.8-81.4 %) and lower silt content (6.5-13 %) compared to the OS subsites (61-71.7 % sand and 19.4-28.2 % silt). The clay content was more or less similar between both sites (7.5-14.8 %) (Table 1). The gravimetric soil water content in KH ranged from 28.0 % (of the wet weight) in the dry plots, to 63.4 % in the intermediate plots and 70.0 % in the wet plots (Table 1). The high difference in water content might be explained by the lower amount of clay in the dry plots compared to the intermediate and wet plots. In OS, the soil water content along the moisture gradient was generally lower due to its elevation. While the dry plots exhibited 23.5 % of soil water content, the intermediate and wet plots had 34.2 and 48.3 %, respectively (Table 1). Except for the dry plots in KH, which had a soil pH of 5.5, the intermediate and wet plots exhibited pH-values between 6.8 and 7.1, respectively. In OS, the pH in the dry plots was with 7.1 higher compared to the intermediate (6.4) and wet plots (6.9) (Table 1). The soil organic matter (SOM) content was higher in the subsites in KH compared to those in OS. In KH the dry plots exhibited 29.4 % SOM (of the dry weight), whereas the intermediate and wet plots had SOM values of 43.8 and 39.2 %, respectively (Table 1). In contrast, the SOM in OS varied from 12.9 % in the dry plots to 31.4 % in the intermediate plots. Here, the wet plots contained 15.8 % SOM (Table 1). TN values were lower in soil samples in the dry plots of KH and OS (0.66 and 0.34 %, respectively) compared to the intermediate (1.15 and 1.00 %, respectively) and wet (1.06 and 0.50 %, respectively) plots of both sites (Table 1). By contrast, the soil TC values were highest in the intermediate plots. While in KH the TC

content was 22.79 %, OS showed 18.06 %. Soils of the dry plots in both sites contained 13.22 and 6.15 % TC, respectively. The wet plots showed 18.51 % TC in KH and 7.95 % in OS. The TC values well reflected the SOM data (Table 1).

The NH_4-N contents were always higher than those of NO_3-N. The NH_4-N values ranged along the water availability gradient between 30.31 and 49.17 mg kg^{-1} dry weight in KH and between 25.45 and 69.61 mg kg^{-1} dry weight in OS with a tendency of higher amounts in the dry subsites. The NO_3-N contents ranged from 16.24 to 48.65 mg kg^{-1} dry weight in the soil in KH and from 4.97 to 30.71 mg kg^{-1} dry weight in OS. The OS intermediate and wet plots exhibited with 46.78 and 10.34 mg kg^{-1} dry weight much lower values compared to the dry plots (23.62 mg kg^{-1} dry weight) (Table 1). In contrast to both nitrogen compounds, P_{labile} contents were always much lower with values between 3.02 and 4.97 mg kg^{-1} dry weight in KH, and between 1.82 and 2.59 mg kg^{-1} dry weight in OS (Table 1).

The O horizon varied in thickness between 1 and 4 cm among the different plots, i.e. each soil was conspicuously covered by organic material. The depth of the respective soil horizon is given in Table 1. The A horizon consisted mainly of dark decomposed organic materials (humus) and was thinner in KH (>8 and >13 cm) compared with OS (between >20 and >22 cm depth) (Table 1).

Mineralogical soil properties

Quartz was the dominant mineral in all soils, ranging from 47.6 to 73.8 % of the dry weight in KH and from 33.6 to 56.8 % in OS (Table 2). The dry plots in both sites always showed the highest percentage of Quartz (Table 2). Dolomite/Ankerite was the second most abundant mineral and varied between 8.0 and 31.7% of the dry weight in KH and between 4.8 to 22.6% in OS. Na-Plagioclase was present in medium concentrations ranging from 5.0 to 9.2 % at KH, and from 7.1 to 13.3 % at OS. Calcite, Muscovite and Biotite were present in much lower concentrations at KH (0.6 to 3.8 %) compared to OS (3.0 to 12.5 %), while Chlorite and K-Feldspar occurred in low values (Table 2).

Vegetation and cryptogamic cover survey

Biocrusts were the dominant vegetation form in both sites, whereas cyanolichens were sparse (Fig. 4 A, B). In the wet plots of KH up to 40 % of the surface was overgrown by biocrusts. In OS, chlorolichens were the second most dominant functional group, which were twice as abundant compared to KH. Mosses showed a reverse pattern and were the second most abundant vegetation type in KH with an occurrence twice of that in OS. One sixth of the

surface in both sites was covered with vascular plants. Unvegetated area was, however, more dominant than biocrusts in OS, and even twice as abundant in KH (Fig. 4 A).

Vegetation ground cover composition in the dry, intermediate and wet plots significantly differed in each of the two sites, as indicated by pairwise PERMANOVA ($p \leq 0.001$; Fig. 4 B) and nMDS (Fig. 5). In addition, each of the three plots in KH differed significantly from the respective subsite in OS ($p \leq 0.01$). Multivariate analysis of the vegetation classes and the respective soil parameters for each plot in KH and OS revealed that wet plots from both sites were quite similar to each other and dominated by moss (e.g. *Racomitrium lanuginosum*) and biocrusts (Fig. 5). However, large differences in the ground cover composition were observed between the two sites KH and OS for the dry plots and also, although not as prominent, for the intermediate plots.

The dry plots of both catenas were about one third unvegetated (stones, bare soil, litter), while mosses were almost absent. In OS, vascular plants covered another third of the dry area and were three times as common as in KH, where they covered only 10 % of the soil surface. In OS biocrusts and chlorolichens appeared in equal amounts but were a bit scarcer than in KH. In KH, cyanolichens were as numerous as biocrusts and chlorolichens, and three times as frequent as in OS (Fig. 4 B). In the intermediate plots, KH was dominated by biocrusts. Mosses, vascular plants and unvegetated area were equally common, whereas lichens covered a small surface. In OS, ground coverage in the intermediate plots was completely different. It was dominated by vascular plants and unvegetated area. Unlike in KH, cyanolichens but also mosses were scarce. Chlorolichens, however, made up almost one fifth of the total area and were three times as frequent as in the KH intermediate plots (Fig. 4 B). Biocrusts were prevailing in the wet plots of both field sites. Mosses covered about one third of the wet ground in KH, and one fifth in OS. Chlorolichens covered one fifth of the ground in OS, whereas in KH they were negligible. Vascular plants covered one fifth in KH, but were scarce in OS. Cyanolichens were almost absent in both field sites (Fig. 4 B). In summary, a significant shift in ground cover composition could be observed along the catenas. Based on pairwise PERMANOVA in both field sites KH and OS, biocrusts ($p \leq 0.05$) and mosses ($p \leq 0.001$) increased with increasing soil moisture, whereas cyanolichens ($p \leq 0.05$) and unvegetated area ($p \leq 0.01$) decreased. Chlorolichens also decreased, but this was significant only in KH ($p \leq 0.001$). In OS, vascular plants decreased with increasing soil moisture ($p \leq 0.001$), while only an increasing yet statistically insignificant trend ($p > 0.05$) was observed in KH.

Three soil parameters were significantly correlated with the change in the vegetation cover (PERMANOVA), namely moisture (explained variance: 30 %, p=0.001), pH (explained variance: 20.5 %, p=0.002) and ammonium concentration (explained variance: 13 %, p=0.012).

Altogether, 24 different vascular plant species belonging to 11 families could be observed (Table 3). Six of these were present in both field sites, 14 species were exclusive to KH, and four species were only observed in OS (Table 3, Fig. 6). In KH, the species richness was higher in the dry and intermediate plot (13 species) compared to the wet plot (nine species). In OS, all plots harbored six to seven different plant species (Table 3, Fig. 6). The dwarf shrubs *Saxifraga oppositifolia* and *Salix polaris* were present in both study sites and almost all plots, whereas the graminoid *Luzula nivalis*, as well as the forbs *Cerastium arcticum, Draba alpine, Minuartia rubella, Papaver dahlianum* and *Pedicularis hirsuta* could only be observed in the dry plot of KH (Online Resource 1). A summarizing scheme of both Arctic vegetation toposequences along the catenas and soil moisture gradients in KH and OS is shown in Figure 7.

Discussion

Soil properties - carbon

Soil organic matter (SOM) values along both moisture availability gradients ranged between 29.4 and 43.8 % of the dry weight in KH, and between 12.9 and 31.4 % in OS. Interestingly, the intermediate plots had higher SOM values compared to the wet and dry sites. This is in agreement with studies from Arctic tundra soils in northern Alaska (Mercado-Díaz et al. 2014) and central Northwest Territories in Canada (Chu and Grogan 2010), which reported similar SOM values of 29.2-34.9 % and 34.5-46.5% SOM, respectively. The corresponding TC contents for each plot were always approximately half of those of the SOM (Table 1). Arctic tundra vegetation is characterized by a significant transfer of fixed C below ground into storage organs (e.g. roots, rhizomes, tillers etc.) at the end of the growing season as part of their energy conservation and overwintering mechanism. Consequently, most of the plant C ends up in the soil (e.g. through litter or exudates), where it is recycled through microbiological activity, gradually being released by respiratory processes and thus returning to the atmosphere. Therefore, high vegetation coverage leads to enhanced SOM accumulation. However, the process of decomposition in the Arctic is generally very slow, mainly because of low temperatures, as well as due to a lack of moisture in well drained soils or excess water where drainage is inhibited (Harden et al. 2012). Plant-derived SOM gradually accumulates,

forming more mature soils, or in wetlands such as bogs, lack of oxygen through waterlogging, causes formation as peat.

Soil properties - nitrogen

In contrast to the large amount of soil organic C, Arctic soils store 8-15 Gt N which equals about 10 % of the global soil N content (Loisel et al. 2014). The TN contents in the present study ranged between 0.34 and 1.15 % of the soil dry weight with concomitant rather low NH_4-N (31.25 – 56.89 mg kg^{-1} soil dry weight) and NO_3-N (6.78 – 29.84 mg kg^{-1} soil dry weight) amounts (Table 1), which are comparable to both nutrients in the Canadian tundra (Chu and Grogan 2010) and in cryosols from Siberia and Greenland (Wild et al. 2013). The C/N ratio (calculated from Table 1) ranged between 16 and 20, and indicated clear N limitation at all study sites, because the typical C/N stoichiometry for soils on a global scale is around 14 and those of soil microbial biomass between 8 and 9 (Cleveland and Liptzin 2007). The data of the present study agrees with Chapin et al. (2011) who assumed that N limitation is most common in Arctic ecosystems. The C/N was lowest at both wet study plots (16 to 17) compared to the dry and intermediate test plots with a C/N ratio of 18 to 20. As mineralization rates are generally low in Arctic biomes, only small proportions of this N are bioavailable (Wild et al. 2013). In addition, N availability also controls rates, directions and magnitudes of C fluxes in Arctic ecosystems under increasing warming (Chu and Grogan 2010), i.e. the soil C- and N-cycle are strongly interlinked. Recently, NO_3-N was reported to be an important N source for Arctic tundra plants (Lui et al. 2018). Consequently, the intermediate plot of OS with the lowest NO_3-N content (6.78 mg kg^{-1} soil dry weight) (Table 1), might have the strongest N limitation for decomposition. This is in agreement with the largest SOM (31.4 %) accumulation at this plot within the OS area. Microbial mineralization of SOM is regarded as a main source for the annual N mobilization in Arctic soils (Schimel and Bennett 2004), which is supplemented by the biological fixation of atmospheric N (Hobara et al. 2006), as well as by atmospheric deposition of inorganic N compounds (Van Cleve and Alexander 1981). Nevertheless, the annual N-requirements of the Arctic vegetation is about 2-3 times higher compared to all N-mobilization and input processes (Shaver and Chapin 1991), which supports the general view of N-limitation of Arctic vegetation (Reich et al. 2006). However, many of the calculations on N-budgets in Arctic soils were undertaken rather locally and already decades ago, and hence do not well reflect recent environmental changes in the tundra.

Soil properties - phosphorus

Although P is at least as important as N for the Arctic tundra vegetation (Giesler et al. 2012; Zamin and Grogan 2012) and soil microorganisms (Gray et al. 2014), it is not well understood how much P is available in Arctic soils. The present study revealed very low available P contents in Svalbard soils, ranging from only 1.8 to 5.0 mg kg^{-1} dry weight (Table 1). Other Arctic soils such as in Canada or Alaska contain much higher P amounts between 17 and several hundred mg kg^{-1} dry weight (Mercado-Díaz et al. 2014; Keller et al. 2007). Chemical and biological weathering of primary minerals like apatite is the main input of P in Arctic soils. This difference between our sites and other regions might thus be related to the soil mineral composition. In both KH and OS, the mineral composition is dominated by quartz, chlorite and plagioclase which are minerals lacking P. More detailed studies on biogeochemical cycling and budgets of P in Arctic soils are urgently needed.

Vegetation and cryptogamic cover survey along the catenas

The catenas in KH and OS differed in their overall areal cover by functional vegetation types (Fig. 4). Moisture content reflecting the local topography was significantly related to these community changes in vegetation (Fig. 5). Soil moisture in summer is mainly dependent on the soil structure, thawed permafrost layer and height above the water level in our catenas (permanent lake in OS, wetland in KH), since precipitation at that season is low (see Material and Methods) and melt water is only important in May and June. According to Elvebakk (1999), Arctic vegetation and topography are strongly correlated, since topography, influences water availability, in particular water runoff, which itself is strongly influenced by the vegetation type. Cryptogamic covers, in particular biocrusts and lichens, shape the soil surface by protecting fine-grained material from water erosion, thereby acting as water barriers for the underground layers leading to a higher runoff while mosses more likely trap water. Further, it is important to mention, that rooting depth of vascular plants is limited in Arctic soils because of permafrost and the relatively low A-horizon (maximum depth in KH 13 cm, in OS 22 cm; Table 1), thus, mainly top soil moisture content shapes the vegetation.

A complete High Arctic toposequence consists of dry exposed ridges, mesic slopes and zonal snow beds, and ends up in a wet area. From the exposed ridge to the wet site, soil moisture increases, which affects the vegetation. Ridges and slopes are dominated by prostrate dwarf shrubs and rosette herbs, snow beds by forbs, and wet sites by mosses, grasses and sedges. Moreover, with increasing water availability, the vegetation becomes denser (Elvebakk 1999; Walker 2000). Apart from some small differences, we found a more or less similar vegetation

pattern in our study sites (Fig. 7). Herbs and lichens dominated the dry plots in KH, while prostrate dwarf shrubs were almost completely absent, which are the prevailing vegetation type on exposed ridges and mesic slopes according Elvebakk (1999). The absence of prostrate dwarfs in KH is likely related to the toposequence starting directly with a snow bed rather than an exposed ridge or a mesic slope. In addition, the intermediate plots all lie within the same topographic entity as the wet site. This is reflected in a similar vegetation composition, which is dominated by mosses and biocrusts (Fig. 7) and the lack of a significant increase in moisture content from the intermediate to the wet plots (Table 1).

In contrast to KH, OS exhibited a complete High Arctic toposequence, consisting of exposed ridges, mesic slopes and zonal snow beds ending up in a wet area along the moisture transect (Elvebakk 1994). The prostrate dwarf shrubs such as *Dryas octopetala* and *Cassiope tetragona*, which are typical for exposed ridges and slopes, dominated the plant communities in the dry and intermediate plots. Biocrusts, mosses and lichens were the dominant vegetation in the wet plots (Fig. 7). These vegetation patterns are well reflected in the moisture content of the top soils (Table 1), as the soil water content significantly increased from the dry to the intermediate plots in both field sites. The dominance of cyanobacteria-dominated biocrusts at the wet plots can be explained by the dominant form of atmospheric water supply being a key driver of biocrust community structure - while terrestrial green algae can use water vapor as the only water source, liquid water (rain or melt water) is a prerequisite for the development of cyanobacteria (Lange et al. 1986).The conspicuously different vegetation between KH and OS can be explained by differences in the toposequence including site-specific physical and chemical parameters, but also by regional microclimatic conditions as a result of the difference in exposure of the transects. KH is an open plain with the glaciers Vester Brøggerbreen and Mørebreen to the South and West, and Kongsfjorden to the North. Strong katabatic winds from the glaciers towards the sea are quite common and likely have a cooling effect on this study site. OS on the other hand is relatively sheltered by surrounding mountain ridges and hence might have a milder climate than KH. This is also evident from differences in the vascular plant species composition between both sites. More in particular, OS is protected as a nature reserve because it is the most northern limit of a number of vascular plants (e.g. *Comastoma tenellum*, *Tofieldia pusilla*) in Svalbard as a result of its particular microclimatic conditions (Birkeland et al. 2017).

The plant community around Ny-Ålesund (including KH) was described as the *Cetrariella delisei-Saxifraga oppositifolia* association within the *Luzulion nivalis* alliance (Elvebakk 1994; Øvstedal et al. 2009). In the dry plots of KH, *Saxifraga oppositifolia* and a lichen

strongly resembling *Cetrariella delisei* indeed grew extensively. For OS, the *Dryado-Caricetum rupestris* and *Cassiopo tetragonae-Dryadetum octopetalae* associations were reported (Elvebakk 1994). Both associations belong to the *Caricion nadinae* alliance and are typical for exposed ridges and mesic slopes, respectively (Elvebakk 1994). These findings are in accordance with the vegetation in OS: *D. octopetala* and *Carex rupestris* appeared to be very numerous in the dry plots, and *Cassiope tetragona* and *D. octopetala* in the intermediate plots. Hence, a *Dryado-Caricetum rupestris* association in the dry plots seems to shift towards a *Cassiopo tetragonae-Dryadetum octopetalae* association in the intermediate plots along the OS transect. All vegetation communities found in KH and OS prefer slightly acidic to slightly alkaline substrate (Elvebakk 1994; Øvstedal et al. 2009), which corresponds to the measured pH values from soils along the transect (Table 1).

Chlorolichens were generally more abundant then cyanolichens and covered up to 20 % of the dry plots in KH, which is in agreement with other sites on Svalbard (Williams et al. 2017). Both lichen groups differ in their ecosystem functions. Chlorolichens are known as soil stabilizer and effective preventer of soil erosion, as high primary producer already under high air humidity alone and producer of C-rich metabolites that can be leached into the soil (Williams et al. 2017). In contrast, cyanolichens are less effective soil stabilizer, which typically exhibit high primary production under liquid water conditions, and which leach N-rich metabolites into the soil (Williams et al. 2017). The low precipitation in the Ny-Ålesund region and lack of melt water during the summer season thus explains the higher abundance of chlorolichens over cyanolichens. Similar lichen patterns were described for the west coast of Greenland (Heindel et al. 2019). Typical chlorolichen taxa associated with biocrusts are *Cetraria muricata*, *Cladonia pyxidata*, *Lepraria* cf. *neglecta*, and *Psora rubiformis*, which are part of the about 600 known lichen species of the flora of Svalbard (Elvebakk and Hertel 1997). However, these lichen numbers are based on total numbers and not only those associated with biocrusts.

Our most intriguing observation was that intermediate and wet plots in KH and the wet plots in OS were dominated by biocrusts and mosses. This would assign these plots to a wetland association. However, the Svalbard wetland vegetation is poorly studied and biocrusts have not been included into its flora characterization (Elvebakk 1994; Walker et al. 2009). Therefore, we propose the integration of biocrusts into vegetation associations in the form of a new syntaxon. The already used terms ‘lichen’, ‘bryophyte’, and ‘cryptophyte’ (Weber et al. 2000) should be modified to ‘lichen’, ‘moss’ and ‘biocrust’ to define the vegetation in a more

realistic and consistent way, as they are clearly too abundant in the Arctic tundra to be neglected.

Although biocrusts were the dominating vegetation type in the wet plots, only dark biocrusts were detected. The missing light biocrusts are defined as an early developmental stage with low biodiversity (Pushkareva et al. 2016). The dominant phototrophic organisms in light biocrusts are filamentous green algae and cyanobacteria. These communities stabilize the soil beneath and thereby facilitate the colonialization by other non-filamentous microalgae and cyanobacteria (Weber et al. 2016). Dark biocrusts are at a later successional stage and possess a higher biodiversity (Weber et al. 2016). The substrate stability and properties due to colonialization by biocrusts is fundamental for the even later succession of mosses, lichens and ultimately vascular plants (Breen and Levesque 2006; Langhans et al. 2009). This has been shown in a vegetation study of a glacier foreland on Svalbard which ran for over 40 years and showed that biocrusts were eventually replaced by vascular plants (Hodkinson et al. 2003). Dark biocrusts were common in both field sites (14 % in OS, 42 % in KH). This indicates well-developed biocrusts in the studied sites (Pushkareva et al. 2016) which in turn reflects low disturbance by mechanical processes like cryoturbation (Pushkareva et al. 2016; Yoshitake et al. 2010).

Conclusions

Our findings highlight the importance of cryptogamic covers in Arctic tundra, which have been largely neglected in earlier vegetation surveys. We suggest that besides lichens and mosses, in particular biocrusts should be considered as a new additional syntaxon in future Arctic vegetation mapping. In the face of global change particularly at high latitudes we further suggest that long-term studies of the dynamics in the vegetation composition are necessary to better understand the crucial role cryptogamic covers and in particular biocrusts play in the ‘greening of the Arctic’. In addition, soil moisture could be identified as an ecological key factor controlling vegetation type and coverage.

Author Contributions

RK, VH, AF, BT, DV, CS, BF, EV, AQ, MS, KG and UK all contributed to the study design as well as sample and data collection during the joint summer expedition 2017 in Ny-Ålesund. MA, CB, MP, AF and LDM analyzed samples for specific parameters. RK, VH, KG and UK undertook all statistical analysis. RK, VH and UK wrote the first version of the manuscript with contributions from all coauthors.

Funding

This study was funded through the 2015-2016 BiodivERsA COFUND call for research proposals, with the national funders of Belgium (BELSPO BR/175/A1/CLIMARCTIC-BE), Germany (DFG KA899/33-1), Norway (The Research Council of Norway 270252/E50), Spain (MINECO, PCIN2016-001, CTM2016-79741) and Switzerland (SNSF 31BD30_172464).

Conflict of Interest Statement

The authors declare that the research was conducted in the absence of any commercial or financial, as well as non-financial relationships that could be construed as a potential conflict of interest.

Acknowledgements

The authors are grateful to the staff at the AWIPEW station, Ny-Ålesund for excellent technical and logistic support during the summer campaign 2017.

Electronic Supplementary Material

The Electronic Supplementary Material for this article can be found as Online Resource 1 and 2:

References

Berg G, Smalla K (2009) Plant species and soil type cooperatively shape the structure and function of microbial communities in the rhizosphere. FEMS Microb Ecol 68:1-13. doi:10.1111/j.1574-6941.2009.00654.x

Birkeland S, Skjetne IEB, Brysting AK, Elven R, Alsos IG (2017) Living on the edge: conservation genetics of seven thermophilous plant species in a high Arctic archipelago. AoB PLANTS 9:plx001. doi:10.1093/aobpla/plx001

Breen K, Levesque E (2006) Proglacial succession of biological soil crusts and vascular plants: biotic interactions in the High Arctic. Can J Bot 84:1714–1731. doi.org/10.1139/b06-131

Castillo-Monroy A, Maestre F, Delgado-Baquerizo M, Gallardo A (2010) Biological soil crusts modulate nitrogen availability in semi-arid ecosystems: insights from a

Mediterranean grassland. Plant Soil 333:21–34. doi.org/10.1007/s11104-009-0276-7, 2010.

Chapin III FS, Shaver GR (1981) Changes in aoil properties and vegetation following disturbance of Alaskan Arctic tundra. J Appl Ecol 18:605-617. doi: 10.2307/2402420

Chu H, Grogan P (2010) Soil microbial biomass, nutrient availability and nitrogen mineralization potential among vegetation-types in a low Arctic tundra landscape. Plant Soil 329:411-420. doi.org/10.1007/s11104-009-0167-y

Cleveland C, Liptzin D (2007) C:N:P stoichiometry in soil: is there a “Redfield ratio” for the microbial biomass? Biogeochem 85: 235-252. doi 10.1007/s10533-007-9132-0Döbelin N, Kleeberg R (2015) Profex: a graphical user interface for the Rietveld refinement program BGMN. J Appl Crystal 48:1573-1580. doi.org/10.1107/S1600576715014685

Dusa A (2017) Venn: Draw Venn Diagrams.

Edwards KA, Jefferies RL (2013) Inter-annual and seasonal dynamics of soil microbial biomass and nutrients in wet and dry low-Arctic sedge meadows. Soil Biol Biochem 57:83-90. doi.org/10.1016/j.soilbio.2012.07.018

Elbert W, Weber B, Burrows S, Steinkamp J, Büdel B, Andreae MO, Pöschl U (2012) Contribution of cryptogamic covers to the global cycles of carbon and nitrogen. Nat Geosci 5:459-462. doi.org/10.1038/ngeo1486, 2012.

Elvebakk A (1994) A survey of plant associations and alliances from Svalbard. J Veg Sci 5:791-802. doi.org/10.2307/3236194

Elvebakk A, Hertel H (1997) A catalogue of Svalbard lichens. In Elvebakk A, Prestrud P (eds) A catalogue of Svalbard plants, fungi, algae, and cyanobacteria, Norsk Polarinstitutt Skrifter, Oslo, Norway, pp 271-411.

Elvebakk, A. (1999). Bioclimatic delimitation and subdivision of the Arctic. In: Nordal I, Razzhivin VY (eds) The species concept in the High North — A Panarctic Flora Initiative. The Norwegian Academy of Science and Letters, Oslo, Norway, pp 81–112.

Gee GW, Bauder JW (1986) Particle-size analysis. In: Klute A (ed) Methods of soils analysis, part 1: Physical and mineralogical methods. Agronomy Monograph, 9, 2nd ed. American Society of Agronomy/Soil Science Society of America, Madison, WI, USA, pp 383-411.

Giesler R, Esberg C, Lagerström A, Graae BJ (2012) Phosphorus availability and microbial respiration across different tundra vegetation types. Biogeochem 108:429–445. doi.org/10.1007/s10533-011-9609-8

Gray ND, McCann CM, Christgen B, Ahammad SZ, Roberts J, Graham DW (2014) Soil geochemistry confines microbial abundances across an Arctic landscape; implications for net carbon exchange with the atmosphere. Biogeochem 120:307–317. doi.org/10.1007/s10533-014-9997-7

Harden JW, Koven CD, Ping CL, Hugelius G, McGuire AD, Camill P, Jorgenson T, Kuhry P, Michaelson GJ, O'Donnell JA, Schuur EAG, Tarnocai C, Johnson K, Grosse G (2012) Field information links permafrost carbon to physical vulnerabilities of thawing. Geophys Res Lett 39:L15704. doi:10.1029/2012GL051958

Hedley MJ, Stewart JWB, Chauhan BS (1982) Changes in inorganic und organic soil-phosphorus fractions induced by cultivation practices and by laboratory incubations. Soil Sci Soc Am J 46:970-976. doi:10.2136/sssaj1982.03615995004600050017x

Heindel RC, Governali FC, Spickard AM, Virginia RA (2019) The role of biological soil crusts in nitrogen cycling and soil stabilization in Kangerlussuaq, West Greenland. Ecosystems 22:243-256. doi.org/10.1007/s10021-018-0267-8

Hervé M (2018) RVAideMemoire: Testing and Plotting Procedures for Biostatistics. R package version 0.9-69

Hobara S, Mccalley C, Koba K, Giblin AE, Weiss MS, Gettel GM, Shaver GR (2006) Nitrogen fixation in surface soils and vegetation in an Arctic tundra watershed: a key source of atmospheric nitrogen. Arct Antarct Alp Res 38:363–372. doi.org/10.1657/1523-0430(2006)38

Hodkinson ID, Coulson SJ, Webb NR (2003) Community assembly along proglacial chronosequences in the high Arctic: vegetation and soil development in north-west Svalbard. J Ecol 91:651-663. doi.org/10.1046/j.1365-2745.2003.00786.x

Johansen BE, Tømmervik H, Karlsen SR (2012) Vegetation mapping of Svalbard utilizing Landsat TM/ETM+ data. Polar Rec 48:47-63. doi.org/10.1017/S0032247411000647

Johansen BE, Tømmervik H (2014) The relationship between phytomass, NDVI and vegetation communities on Svalbard. Int J Appl Earth Obs 27:20-30. doi.org/10.1016/j.jag.2013.07.001

Keller K, Blum JD, Kling GW (2007) Geochemistry of soils and streams on surfaces of varying ages in Arctic Alaska. Arct Antarct Alp Res 39:84-98. doi.org/10.1657/1523-0430

Lange OL, Kilian E, Ziegler H (1986) Water vapor uptake and photosynthesis of lichens: performance differences in species with green and blue-green algae as phycobionts. Oecologica 71:104-110. doi.org/10.1007/BF00377327

Langhans TM, Storm C, Schwabe A (2009) Community assembly of biological soil crusts of different successional stages in a temperate sand ecosystem, as assessed by direct determination and enrichment techniques. Microb Ecol 58:394-407. doi.org/10.1007/s00248-009-9532-x

Levy E, Madden E (1933). The point method of pasture analysis. New Zeal J Agr Res 46:267–279.

Loisel J, Yu Z, Beilman DW, Camill P, Alm J, Amesbury MJ, Anderson D, Andersson S, Bochicchio C, Barber K, Belyea LR, Bunbury J, Chambers FM, Charman DJ, De Vleeschouwer F, Fialkiewicz-Kozie B, Finkelstein S, Galka M, Garneau M, Hammarlund D, Hinchcliffe W, Holmquist J, Hughes P, Jones MC, Klein ES, Kokfelt U, Korhola A, Kuhry P, Lamarre A, Lamentowicz M, Large D, Lavoie M, MacDonald G, Magnan G, Makila M, Mallon G, Mathijssen P, Mauquoy D, McCarroll J, Moore TR, Nichols J, O'Reilly B, Oksanen P, Packalen M, Peteet D, Richard PJ, Robinson S, Ronkainen T, Rundgren M, Sannel ABK, Tarnocai C, Thom T, Tuittila ES, Turetsky M, Valiranta M, van der Linden M, van Geel B, van Bellen S, Vitt D, Zhao Y, Zhou W (2014) A database and synthesis of northern peatland soil properties and Holocene carbon and nitrogen accumulation. The Holocene 24:1028–1042. doi.org/10.1177/0959683614538073

Liu XY, Koba K, Koyama LA, Hobbie SE, Weiss MS, Inagaki Y, Shaver GR, Giblin AE, Hobara S, Nadelhoffer KJ, Sommerkorn M, Rastetter EB, Kling GW, Laundre JA, Yano Y, Makabe A, Yano M, Liu CQ (2018) Nitrate is an important nitrogen source for Arctic tundra plants. Proc Natl Acad Sci USA 115:3398-3403.

doi.org/10.1073/pnas.1715382115Mercado-Díaz JA, Gould WA, González G (2014). Soil nutrients, landscape age, and *Sphagno-Eriophoretum vaginati* plant communities in Arctic moist-acidic tundra landscapes. OJSS 4:375-387. doi.org/10.4236/ojss.2014.411038

Murphy J, Riley JP (1962) A modified single solution method for the determination of phosphate in natural waters. Anal Chim Acta 27:31-36. doi.org/10.1016/S0003-2670(00)88444-5

Øvstedal D, Tønsberg T, Elvebakk A (2009) The lichen flora of Svalbard. Sommerfeltia 33:3-393. doi.org/10.2478/v10208-011-0013-5

Oksanen J, Blanchet FG, Friendly M, Kindt R, Legendre P, McGlinn D, Minchin PR, O'Hara RB, Simpson GL, Solymos P, Stevens MHH, Szoecs E, Wagner H (2018) Package 'vegan'. Community Ecology Package. Version 2.5-3.

Pushkareva E, Pessi IS, Willmotte A, Elster J (2015) Cyanobacterial community composition in Arctic soil crusts at different stages of development. FEMS Microbiol Ecol 91:fiv143. doi: 10.1093/femsec/fiv143

Pushkareva E, Johansen JR, Elster J (2016) A review of the ecology, ecophysiology and biodiversity of microalgae in Arctic soil crusts. Polar Biol 39:2227–2240. doi.org/10.1007/s00300-016-1902-5

Reich PB, Hobbie SE, Lee T, Ellsworth DS, West JB, Tilman D, Knops JMH, Naeem S, Trost J (2006) Nitrogen limitation constrains sustainability of ecosystem response to CO_2. Nature 440:922–925. doi.org/10.1038/nature04486

Rønning OI (1996) The Flora of Svalbard, 1st ed. Norwegian Polar Institute, Tromsø, Norway

Schimel JP, Bennett J (2004) Nitrogen mineralization: challenges of a changing paradigm. Ecology 85:591–602. doi.org/10.1890/03-8002

Screen JA, Simmonds I (2010) The central role of diminishing sea ice in recent Arctic temperature amplification. Nature 464:1334-1337. doi:10.1038/nature09051

Shaver GR, Chapin III FS (1991) Production:biomass relationships and element cycling in contrasting Arctic vegetation types. Ecol Monogr 61:1–31. doi.org/10.2307/1942997

Van Cleve K, Alexander V (1981) Nitrogen cycling in tundra and boreal ecosystems. In: Clarke FE, Rosswall T (eds) Terrestrial Nitrogen Cycles, Ecol Bull 33:375-404.

Vimal SR, Singh JS, Arora NK, Singh S (2017) Soil-plant-microbe interactions in stressed agriculture management: a review. Pedosphere 27:177-192. doi:10.1016/S1002-0160(17)60309-6

Walker DA (2000) Hierarchical subdivision of Arctic tundra based on vegetation response to climate, parent material and topography. Glob Change Biol 6:19-34. doi.org/10.1046/j.1365-2486.2000.06010.x

Walker DA, Raynolds MK, Daniëls FJ, Einarsson E, Elvebakk A, Gould WA, Katenin AE, Kholod SS, Markon CJ, Melnikov ES, Moskalenko NG, Talbot SS, Yurtsev BA, and the other members of the CAVM Team (2009) The circumpolar Arctic vegetation map. J Veg Sci 16:267–282. doi.org/10.1111/j.1654-1103.2005.tb02365.x

Weber B, Büdel B, Belnap J (2016) Biological soil crusts: an organizing principle in drylands, 1st ed. Springer, Berlin, Heidelberg, Germany.

Weber HE, Moravec J, Theurillat JP (2000) International Code of Phytosociological Nomenclature, 3rd edition. J Veg Sci 11:739-768. doi.org/10.2307/3236580

Wild B, Schnecker J, Bárta J, Capek P, Guggenberger G, Hofhansl F, Kaiser C, Lashchinsky N, Mikutta R, Mooshammer M, Santracková H, Shibistova O, Urich T, Zimov S, Richter

Formatiert: Englisch (USA)

A (2013) Nitrogen dynamics in turbic cryosols from Siberia and Greenland. Soil Biol Biochem 67:85–93. doi.org/10.1016/j.soilbio.2013.08.004

Williams L, Borchhardt N, Colesie C, Baum C, Komsic-Buchmann K, Rippin M, Becker B, Karsten U, Büdel B (2017) Biological soil crusts of Arctic Svalbard and of Livingston Island, Antarctica. Polar Biol 40:399-411. doi.org/10.1007/s00300-016-1967-1

Yoshitake S, Uchida M, Koizumi H, Kanda H, Nakatsubo T (2010) Production of biological soil crusts in the early stage of primary succession on a High Arctic glacier foreland. New Phytol 186:451-460. doi.org/10.1111/j.1469-8137.2010.03180.x

Zamin TJ, Grogan P (2012) Birch shrub growth in the low Arctic: the relative importance of experimental warming, enhanced nutrient availability, snow depth and caribou exclusion. Environ Res Lett 7:034027. doi.org/10.1088/1748-9326/7/3/034027

Zhang X, Friedl MA, Schaaf CB, Strahler AH (2004) Climate controls on vegetation phenological patterns in northern mid- and high latitudes inferred from MODIS data. Glob Change Biol 10:1133-1145. doi.org/10.1111/j.1529-8817.2003.00784.x

Figure Legends

Fig. 1 A-D. Maps of Svalbard (A, B) and the two study sites Knudsenheia (C) and Ossian-Sarsfjellet (D). The symbols on the magnified maps of Knudsenheia (C) K.1.1. to K.1.3, K.2.1. to K.2.3 and K.3.1 to K.3.3 indicate the dry, intermediate and wet plots, respectively. Accordingly, the symbols on the magnified maps of Ossian-Sarsfjellet (D) O.1.1. to O.1.3, O.2.1. to O.2.3 and O.3.1 to O.3.3 label the dry, intermediate and wet plots, respectively. All plot details are summarized in Table 1.

Fig. 2 A-B. Photographs of the two study sites Knudsenheia (A) and Ossian-Sarsfjellet (B).

Fig. 3. Dendrogram of each replicate from dry (d), intermediate (i) and wet (w) plots from Knudsenheia (KH) and Ossian-Sarsfjellet (OS) based on environmental soil data. The dendrogram was drawn after a cluster analysis using total C/N, labile phosphorus, ammonium, nitrate, pH, moisture, organic matter content and texture of the upper soil samples (Table 1).ediate; KH w: Knudsenheia wet; OS d: Ossian-Sarsfjellet dry; OS i: Ossian-Sarsfjellet intermediate; OS w: Ossian-Sarsfjellet wet.

Fig 4. Summary of the vegetation survey. Percentage of area covered by the different functional groups as determined with the point intercept method on (A) the whole transect and (B) in the subsites along the soil moisture gradient (Data see Table 1). KH: Knudsenheia; OS: Ossian-Sarsfjellet; KH d: Knudsenheia dry; KH i: Knudsenheia intermediate; KH w: Knudsenheia wet; OS d: Ossian-Sarsfjellet dry; OS i: Ossian-Sarsfjellet intermediate; OS w: Ossian-Sarsfjellet wet.

Fig 5. Non-metric multidimensional scaling (nMDS) plot visualizing the similarity and dissimilarity of the ground coverage in Knudsenheia (KH) and Ossian-Sarsfjellet (OS) in the different plots (d-dry, i-intermediate, w-wet). Ellipses correspond to 95% confidence interval. The black arrows indicate the influence direction of the only three significantly correlated soil parameters: ammonium, pH and moisture. Stress=0.15

Fig. 6. Number of vascular plant species (A) in the two field sites and (B) in the subsites. Venn diagram showing the total number of vascular plant species in each field site, Knudsenheia (KH, yellow-brown) and Ossian-Sarsfjellet (OS, turkis-green), as well as the number of species that are present in both sites (intersection). (B) Number of different vascular plant species per plot (dry, intermediate, wet) in Knudsenheia (KH) and Ossian-Sarsfjellet (OS).

Fig. 7. Scheme of both Arctic vegetation toposequences along the soil moisture gradients in Knudsenheia (KH) and Ossian-Sarsfjellet (OS) (d: dry; i: intermediate; w: wet). Only the dominant vegetation is indicated. Adapted after Elvebakk (1994) and Walker (2000).

Figure Legends for Online Resource 1

Fig. 8.1-8.18. Digital photographs of the 18 permanent sampling plots showing the dominant vegetation. K: Knudsenheia; O:Ossian-Sarsfjellet; K1.1-K1.3: dry plots; K2.1-K2.3: intermediate plots; K3.1-K3.3: wet plots; O1.1-O1.3: dry plots; O2.1-O2.3: intermediate plots; O3.1-O3.3: wet plots.

Fig. 9. Non-metric multidimensional scaling (nMDS) plot visualizes the similarity and dissimilarity of the vascular plant diversity in Knudsenheia (KH) and Ossian-Sarsfjellet (OS)

at different plots (d-dry, i-intermediate, w-wet). The black arrows indicate the influence direction of the only three significantly correlated soil parameters: ammonium, pH, sand content and moisture. Ellipses correspond to 95% confidence interval. Stress=0.17

TABLE 1 Plot information and soil properties. Site description including GPS position and elevation are given. All soil parameters were measured in samples from the first centimeter thick soil layer. Moisture (gravimetric soil water content in % of fresh weight), soil organic material (SOM, in % of dry weight, after combustion of dry soil at 450°C) and soil texture (proportion of sand, silt and clay) are given in percent. Total (inorganic and organic) N and C contents of the corresponding nutrient are expressed as percent of dry weight. The soluble nutrients N-NH_4, N-NO_3 and P_{labile} are expressed as mg kg^{-1} dry weight. The grading parameters were measured for at least two pooled subsamples, whereas all other parameters except P_{labile} were analysed for 3 to 8 replicates. The Norwegian Polar Institute provided the elevation data for the different plots. All data represent mean values ± standard deviation. One-way ANOVA was performed to reveal significant differences of the measured soil parameters between the six subsites. Small letters indicate significant differences of each parameter ($p < 0.05$).

Study site	Subsite	Plot	GPS position	Elevation (m)	Soil horizon (cm)	Grading (%) Sand	Silt	Clay	Moisture (%)	pH	SOM (%)	TN (%)	TC (%)	NH_4-N (mg kg^{-1} DW)	NO_3-N (mg kg^{-1} DW)	P_{labile} (mg kg^{-1} DW)
Knudsen-heia	Dry	K1.1	78.93942°N 11.80803°E	36.6	O: 0 - 4	79.5± 4.8^{a}	13.0± 3.4^{a}	7.5± 1.4^{a}	28.0± 9.9^{a}	5.5± 0.2^{a}	29.4± 9.1^{a}	0.66± 0.21^{a}	13.22± 5.0^{a}	42.93± 5.63^{a}	24.28± 12.42^{b}	3.02
		K1.2	78.93948°N 11.80787°E	36.2	OA: 4 - 13											
		K1.3	78.93950°N 11.80762°E	35.8	A: >13											
	Inter-mediate	K2.1	78.93992°N 11.81028°E	31.4	O: 0 - 2	75.8± 10.4^{a}	12.1± 7.2^{a}	13.8± 2.9^{b}	63.4± 9.6^{c}	6.8± 0.1^{b}	43.8± 12.0^{a}	1.15± 0.42^{a}	22.79± 10.7^{a}	40.86± 9.36^{a}	23.28± 6.61^{b}	3.54
		K2.2	78.93995°N 11.81040°E	31.3	OA: 2 - 10											
		K2.3	78.94003°N 11.81147°E	31.1	A: >10											
	Wet	K3.1	78.94180°N 11.82805°E	26.8	O: 0 - 2	81.4± 4.8^{a}	6.5± 1.6^{b}	14.2± 1.1^{b}	70.0± 9.4^{c}	7.1± 0.2^{b}	39.2± 11.9^{a}	1.06± 0.24^{a}	18.51± 4.9^{a}	35.91± 2.85^{a}	29.84± 1.90^{b}	4.97
		K3.2	78.94185°N 11.82793°E	26.7	OA: 2 - 8											
		K3.3	78.94185°N 11.82805°E	26.9	A: >8											
Ossian Sarsfjellet	Dry	O1.1	78.95258°N 12.49257°E	113.2	O: 0 - 1	71.7± 2.8^{a}	19.4± 2.4^{a}	9.2± 0.5^{a}	23.5± 3.4^{a}	7.3± 0.1^{b}	12.9± 4.8^{b}	0.34± 0.06^{b}	6.15± 1.53^{b}	56.89± 16.29^{b}	23.62± 7.92^{b}	1.82
		O1.2	78.95262°N 12.49259°E	113.5	OA: 1 - 20											
		O1.3	78.95272°N 12.49207°E	115.7	A: >20											
	Inter-mediate	O2.1	78.95258°N 12.49368°E	108.1	O: 0 - 4	61.1± 2.3^{b}	24.1± 2.0^{c}	14.8± 3.5^{b}	34.2± 6.2^{a}	6.4± 0.1^{c}	31.4± 10.0^{a}	1.00± 0.23^{a}	18.06± 4.52^{a}	54.31± 1.16^{b}	6.78± 1.88^{a}	2.59
		O2.2	78.95257°N 12.49448°E	105.5	OA: 4 - 22											
		O2.3	78.95257°N 12.49502°E	105.5	A: >22											
	Wet	O3.1	78.95228°N 12.49532°E	100.6	O: 0 - 1	61.0± 3.6^{b}	28.2± 2.4^{c}	10.8± 1.6^{b}	48.3± 5.3^{b}	6.9± 0.5^{b}	15.8± 3.1^{b}	0.5± 0.10^{b}	7.95± 0.71^{b}	31.25± 8.80^{a}	10.34± 4.44^{a}	2.45
		O3.2	78.95228°N 12.49503°E	101.0	OA: 1 - 20											
		O3.3	78.95238°N 12.49632°E	100.7	A: >20											

TABLE 2 Mineralogical soil properties. For sample details see Table 1. Values are given as percentage of dry weight with 3σ error (3 replicates). n.d.: not detected.

Study site	Subsite	Dolomite Ankerite	Calcite	Muscovite	Biotite	Chlorite	Na-Plagioclase	K-Feldspar	Kaolinite	Quartz	Hematite	Sillimanite
Knudsenheia	Dry	8.0±0.9	0.8± 0.1	2.9± 0.2	n.d	5.4± 1.2	5.0± 0.3	1.6± 0.1	1.5± 0.2	73.8± 1.0	1.0± 0.1	n.d.
	Intermediate	31.7±1.5	2.4± 0.2	3.8± 0.2	n.d.	2.4± 0.4	6.9± 0.5	4.0± 0.3	0.6± 0.2	47.6± 0.5	0.6± 0.1	n.d.
	Wet	25.7±0.9	0.6± 0.1	2.4± 0.2	<0.6	2.2± 0.6	9.2± 0.5	3.7± 0.2	n.d	55.6± 0.5	n.d.	n.d.
Ossian Sarsfjellet	Dry	4.8±0.6	6.8± 0.2	6.2± 0.3	3.0± 0.3	3.7± 0.6	13.3± 0.6	5.4± 0.5	n.d	56.8± 0.7	n.d.	n.d.
	Intermediate	10.8±0.6	5.5± 0.2	8.6± 0.3	4.0± 0.5	6.6± 0.6	11.1± 0.7	5.0± 0.4	0.9± 0.3	44.8± 0.6	0.4± 0.1	2.3± 0.3
	Wet	22.6±0.5	12.5± 0.2	9.6± 0.3	5.2± 0.3	5.1± 0.5	7.1± 0.4	3.1± 0.3	1.2± 0.3	33.6± 0.5	n.d.	n.d.

TABLE 3 Plant taxa found at the study sites Knudsenheia (KH) and Ossian Sarsfjellet (OS) along a moisture gradient defined by three subsites dry (d), intermediate (i), and wet (w). The taxonomic level of clade and family for each species is given.

Species	**Family**	**Clade**	**Growth form**	**Occurence**					
				KHd	**KHi**	**KHw**	**OSd**	**OSi**	**OSw**
Equisetum variegatum	Equisetaceae	Equisetopsida	Forb		x				x
Carex sp.	Cyperaceae	Monocotyledonae	graminoid		x	x			
Festuca sp.	Poaceae	Monocotyledonae	graminoid				x	x	
Luzula confuse	Juncaceae	Monocotyledonae	graminoid	x	x				
Luzula nivalis	Juncaceae	Monocotyledonae	graminoid	x					
Poa sp.	Poaceae	Monocotyledonae	graminoid	x			x	x	x
Arenaria sp.	Caryophyllaceae	Dicotyledonae	Forb		x	x			
Bistorta vivipara	Polygonaceae	Dicotyledonae	Forb		x	x			
Cardamine pratensis ssp. *angustifolia*	Brassicaceae	Dicotyledonae	Forb		x	x			x
Cassiope tetragona	Ericaceae	Dicotyledonae	Dwarf shrub					x	x
Cerastium arcticum	Caryophyllaceae	Dicotyledonae	Forb	x					
Draba alpina	Brassicaceae	Dicotyledonae	Forb	x					
Dryas octopetala	Rosaceae	Dicotyledonae	Dwarf shrub				x	x	x
Minuartia rubella	Caryophyllaceae	Dicotyledonae	Forb	x					
Minuartia sp.	Caryophyllaceae	Dicotyledonae	Forb		x	x			
Oxyria digyna	Polygonaceae	Dicotyledonae	Forb	x	x				
Papaver dahlianum	Papaveraceae	Dicotyledonae	Forb	x					
Pedicularis hirsuta	Scrophulariaceae	Dicotyledonae	Forb	x					
Sagina nivalis	Caryophyllaceae	Dicotyledonae	Forb		x	x			x
Salix polaris	Salicaceae	Dicotyledonae	Dwarf shrub	x	x	x		x	x

Saxifraga cernua	Saxifragaceae	Dicotyledonae	Forb	x	x	x			
Saxifraga cespitosa	Saxifragaceae	Dicotyledonae	Forb	x	x	x			
Saxifraga oppositifolia	Saxifragaceae	Dicotyledonae	Forb	x	x		x	x	x
Silene acaulis	Caryophyllaceae	Dicotyledonae	Forb				x	x	

Supplementary data

TABLE 4 Summary of the vegetation surveys on the individual plots. Percentage of area covered by the different functional vegetation groups as determined with the point intercept method on all plots along the soil moisture gradient (dry, intermediate, wet) at Knudsenheia and Ossian Sarsfjellet.

Study site	Subsite	Plot	Vegetation ground cover (%)				
			Higher plants	Mosses	Lichens	Dark BSCs	Unvegetated
Knudsenheia	Dry	K1.1	25	0	50	10	15
		K1.2	25	1	62	2	10
		K1.3	15	1	66	3	15
	Intermediate	K2.1	15	8	5	57	15
		K2.2	40	20	4	30	6
		K2.3	8	5	15	50	22
	Wet	K3.1	7	8	16	65	4
		K3.2	4	2	4	70	20
		K3.3	4	8	6	67	15
Ossian Sarsfjellet	Dry	O1.1	15	0	1	6	78
		O1.2	45	0	1	10	54
		O1.3	25	0	1	14	60
	Intermediate	O2.1	90	1	3	1	5
		O2.2	55	0	15	5	25
		O2.3	85	1	2	10	2
	Wet	O3.1	2	7	0	65	26
		O3.2	1	3	0	66	30
		O3.3	4	8	8	65	15

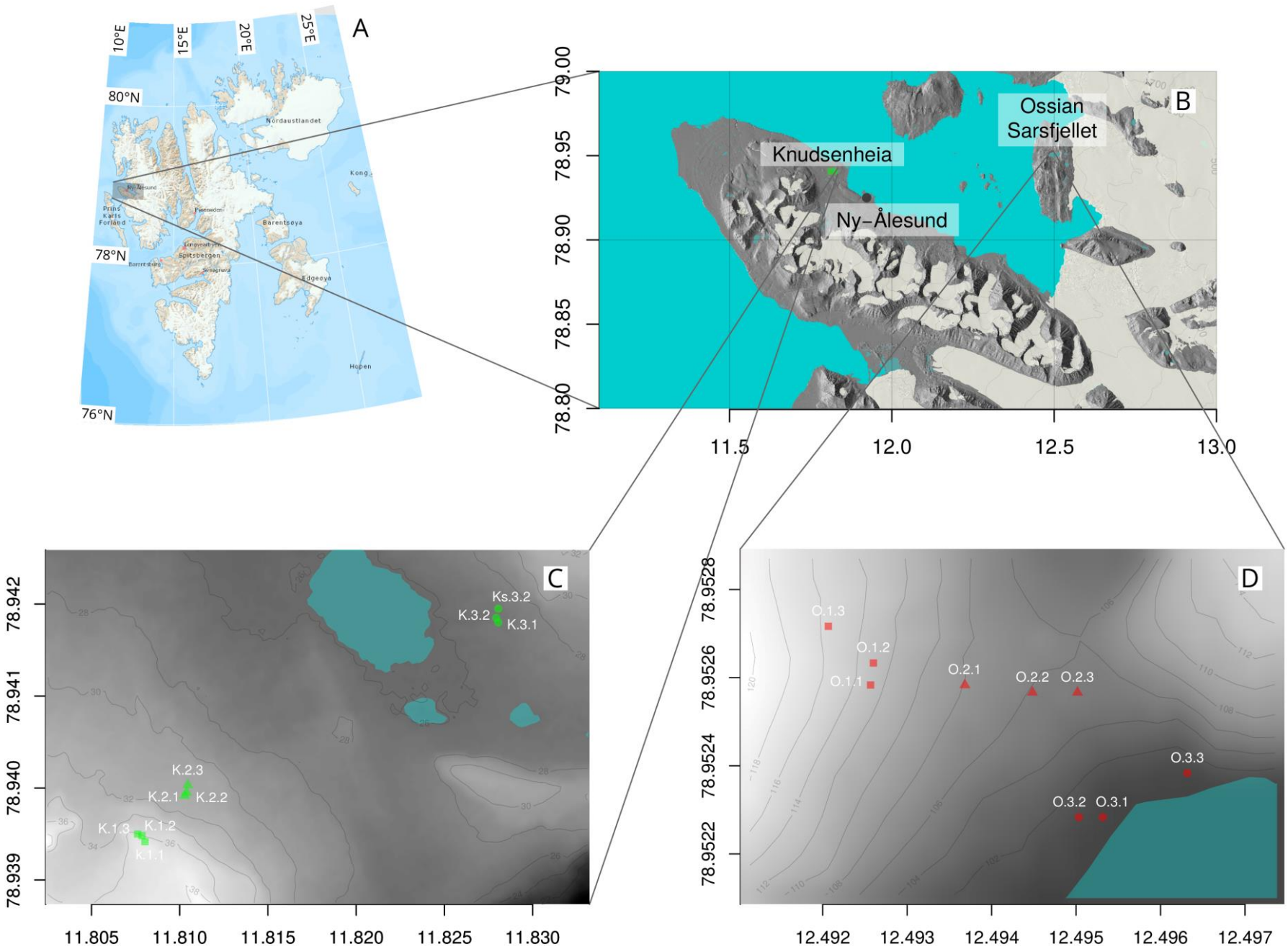
A
10°E
15°E
20°E
25°E
80°N
78°N
76°N
Nordaustlandet
Kong
Ny-Ålesund
Prins Karls Forland
Forlandet
Barentsøya
Spitsbergen
Edgeøya
Hopen
B
Ossian Sarsfjellet
Knudsenheia
Ny-Ålesund
79.00
78.95
78.90
78.85
78.80
11.5
12.0
12.5
13.0
C
Ks.3.2
K.3.2
K.3.1
K.2.3
K.2.1
K.2.2
K.1.3
K.1.2
K.1.1
78.942
78.941
78.940
78.939
11.805
11.810
11.815
11.820
11.825
11.830
D
O.1.3
O.1.2
O.1.1
O.2.1
O.2.2
O.2.3
O.3.3
O.3.2
O.3.1
78.9528
78.9526
78.9524
78.9522
12.492
12.493
12.494
12.495
12.496
12.497

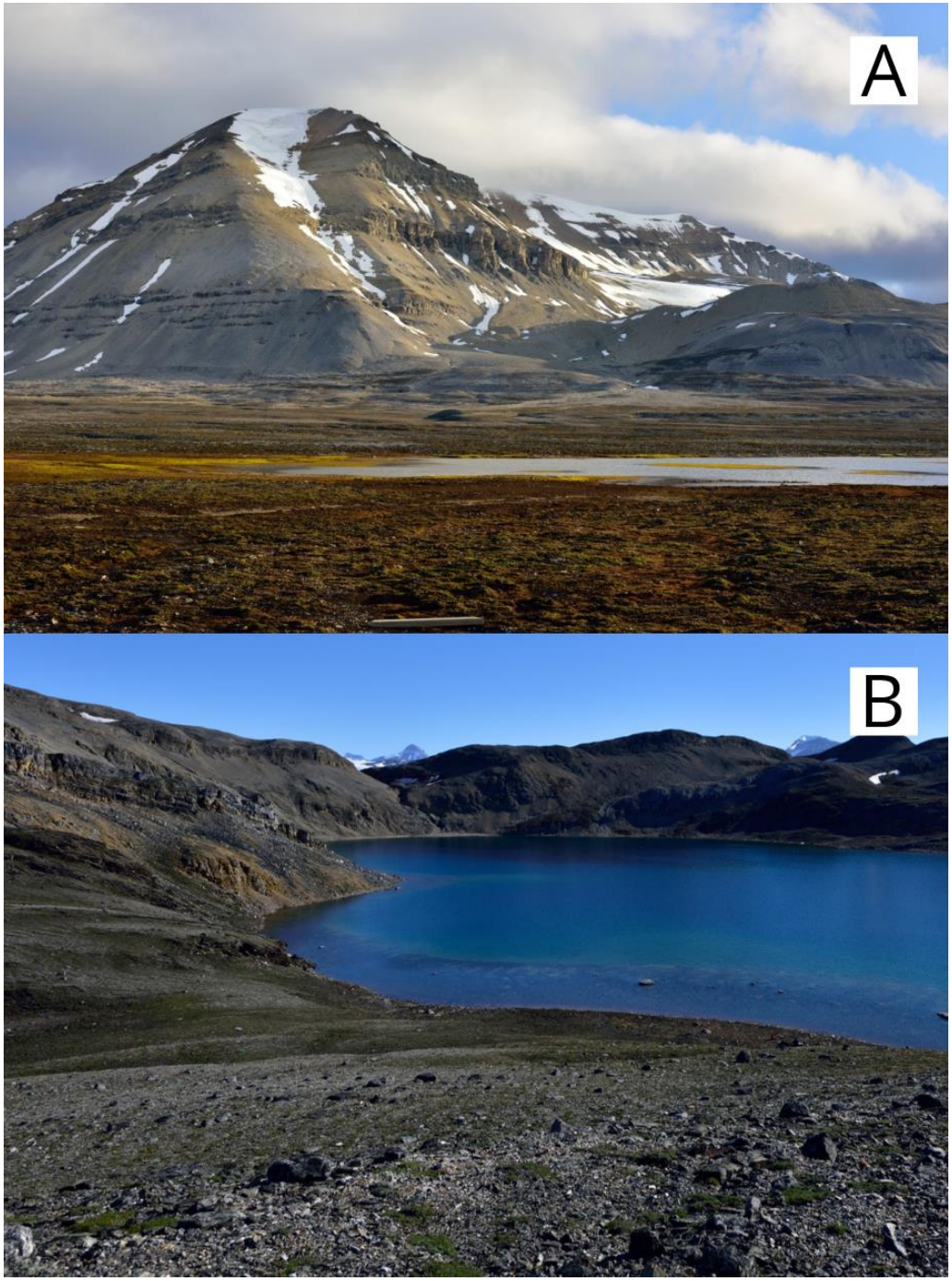
A
B

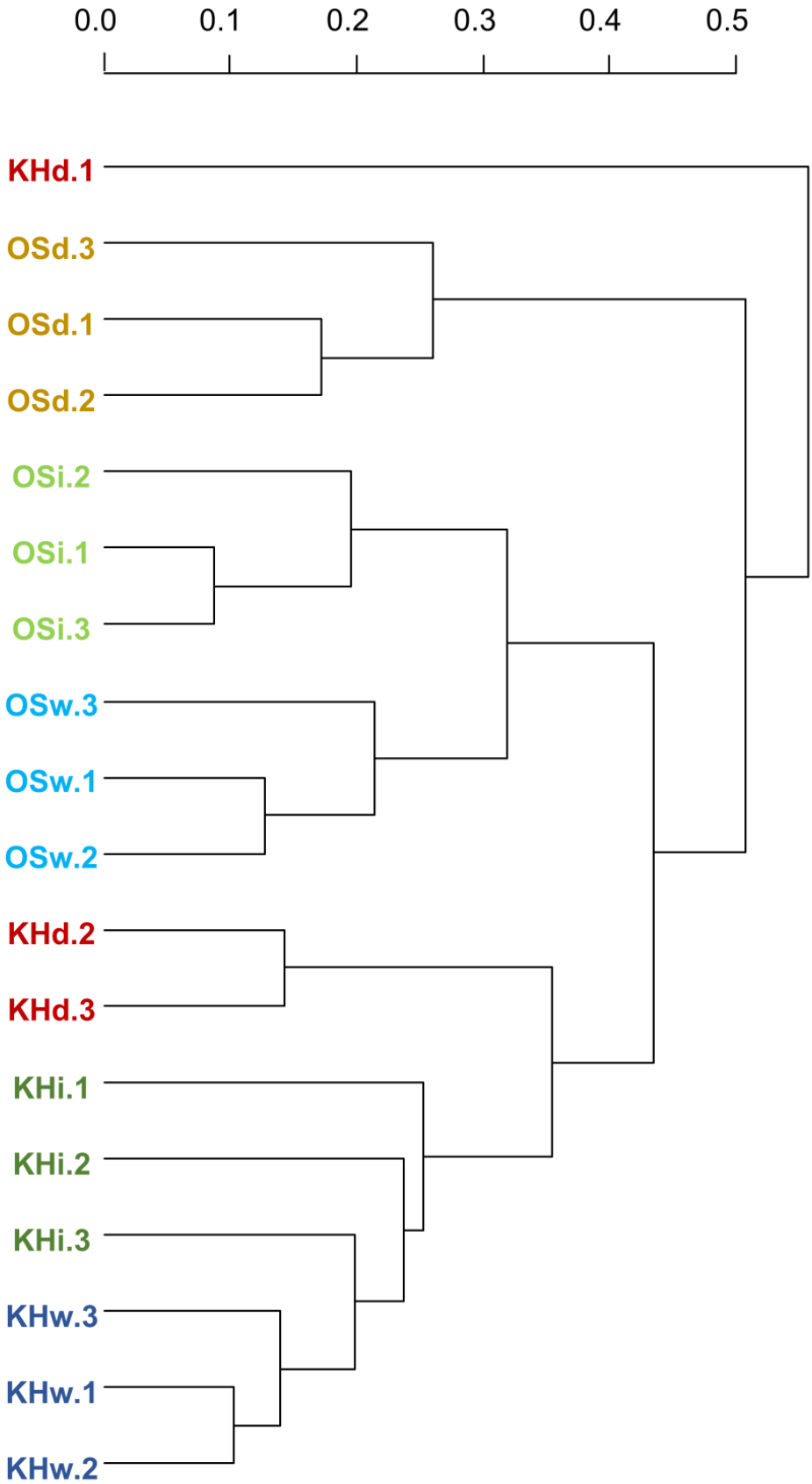
0.0
0.1
0.2
0.3
0.4
0.5
KHd.1
OSd.3
OSd.1
OSd.2
OSi.2
OSi.1
OSi.3
OSw.3
OSw.1
OSw.2
KHd.2
KHd.3
KHi.1
KHi.2
KHi.3
KHw.3
KHw.1
KHw.2

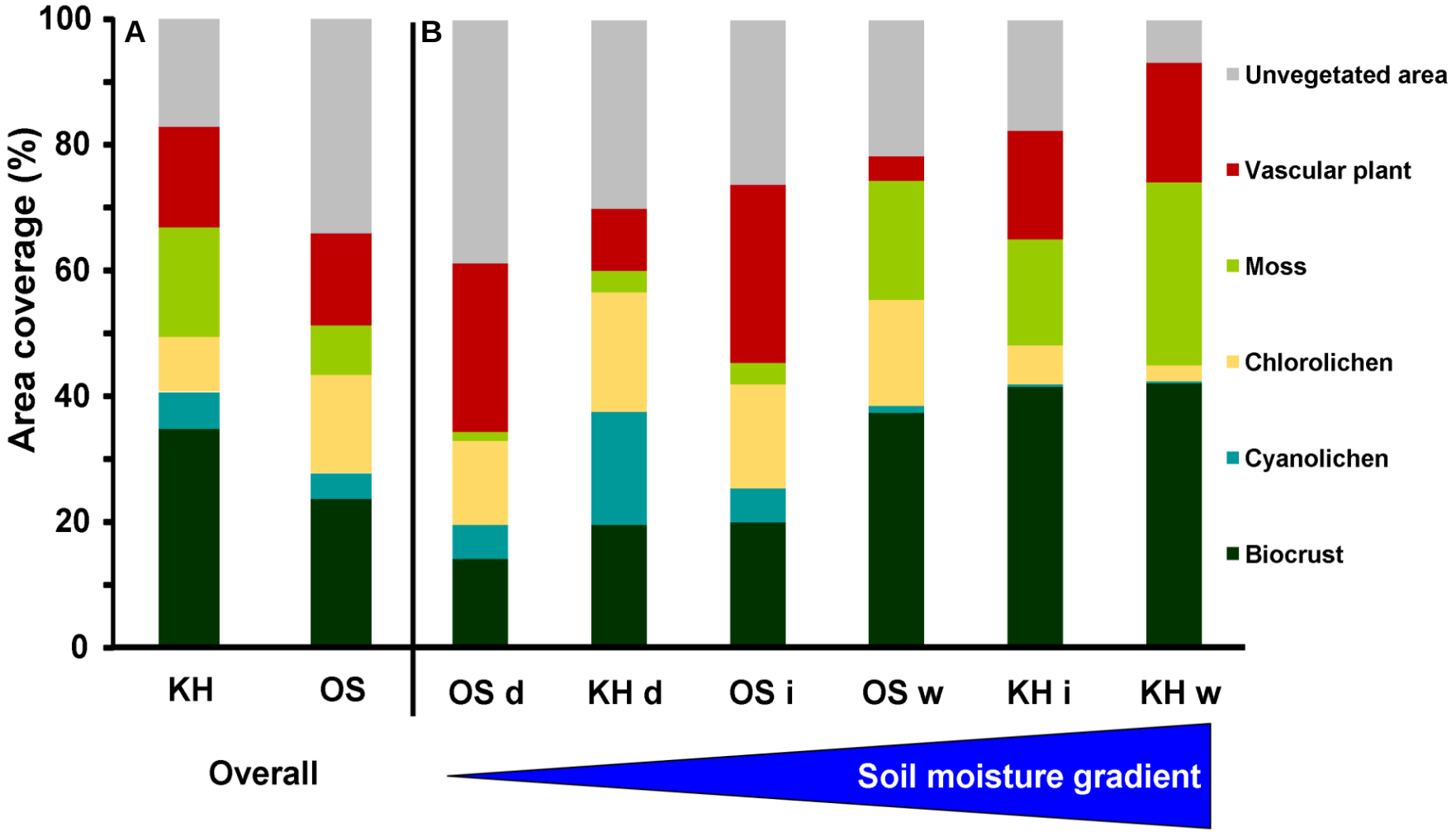
A
B
Area coverage (%)
100
80
60
40
20
0
KH
OS
OS d
KH d
OS i
OS w
KH i
KH w
Overall
Soil moisture gradient
Unvegetated area
Vascular plant
Moss
Chlorolichen
Cyanolichen
Biocrust

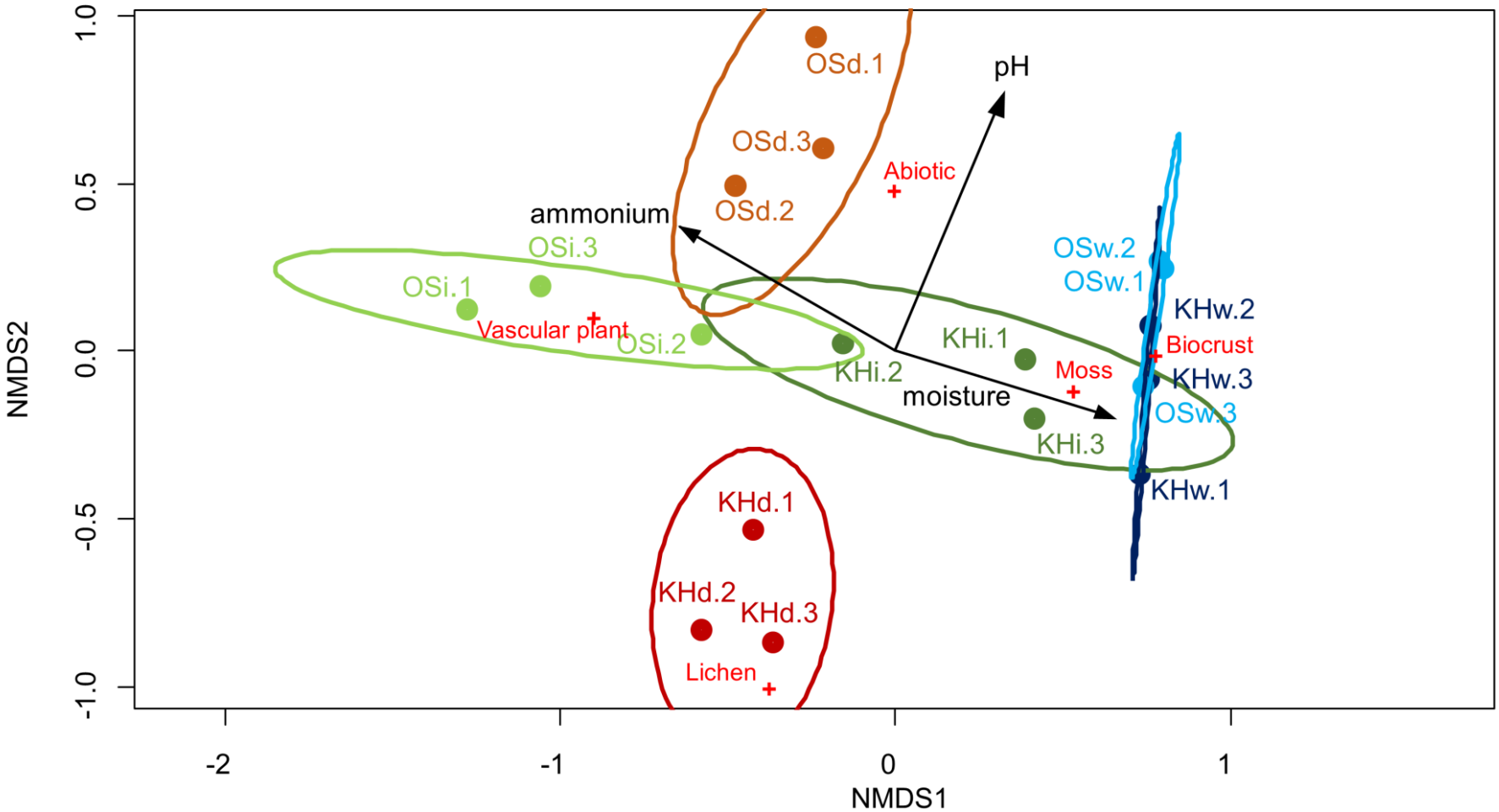
NMDS2
NMDS1
1.0
0.5
0.0
-0.5
-1.0
-2
-1
0
1
OSd.1
OSd.3
OSd.2
pH
Abiotic
ammonium
OSi.3
OSi.1
Vascular plant
OSi.2
OSw.2
OSw.1
KHw.2
Biocrust
KHw.3
OSw.3
KHw.1
KHi.1
Moss
KHi.2
moisture
KHi.3
KHd.1
KHd.2
KHd.3
Lichen

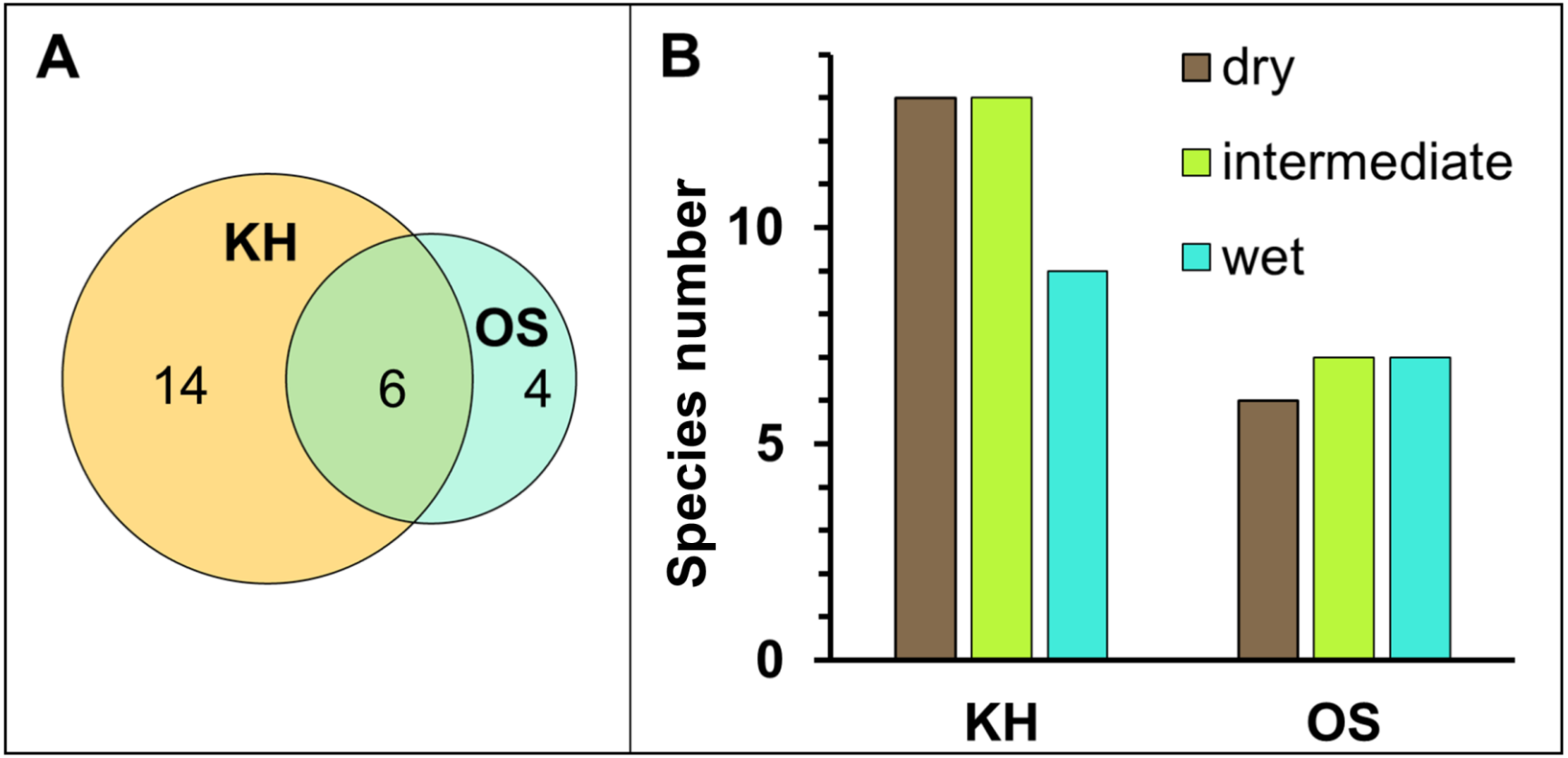
A
KH
OS
14
6
4
B
dry
intermediate
wet
Species number
0
5
10
KH
OS

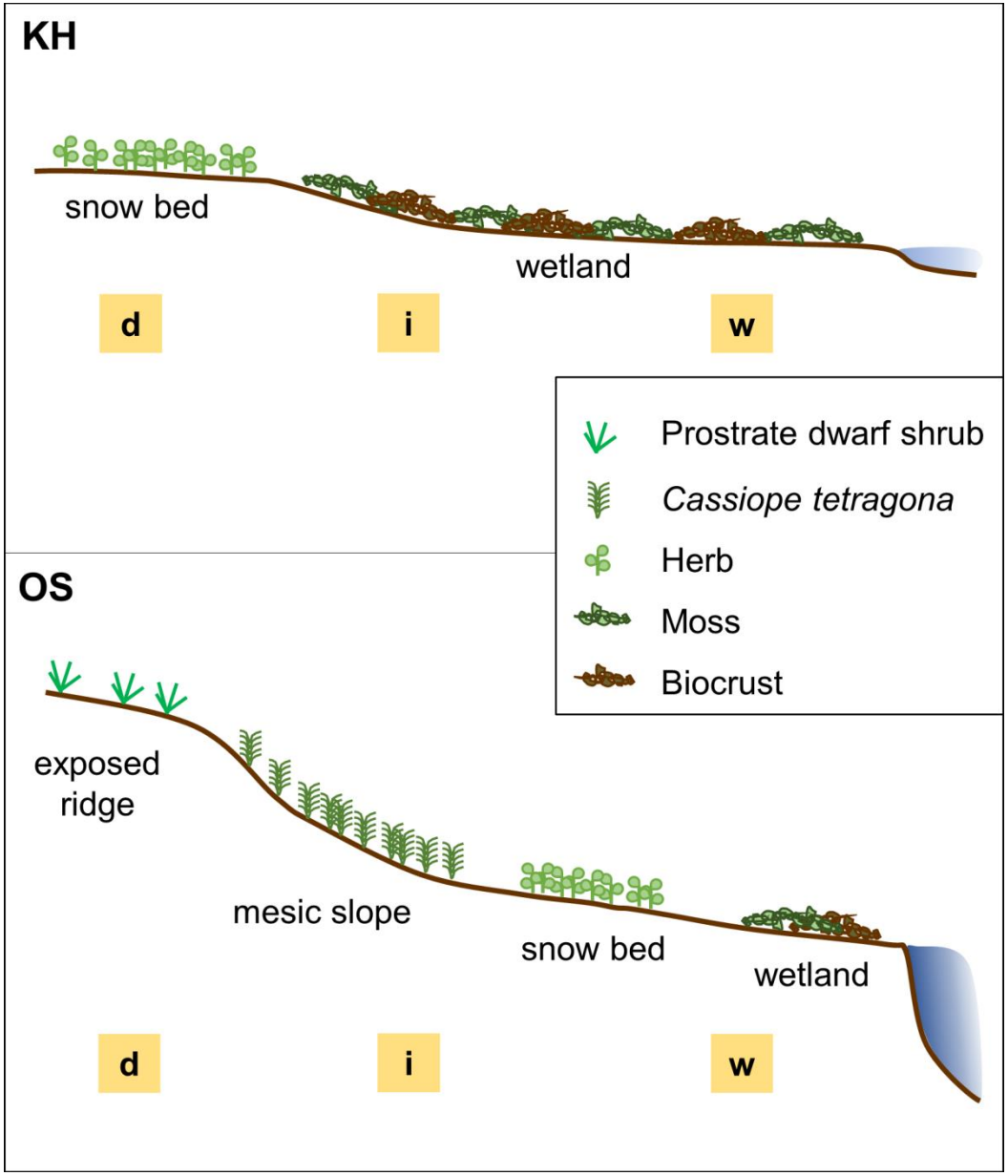
KH
snow bed
wetland
d
i
w
Prostrate dwarf shrub
Cassiope tetragona
Herb
Moss
Biocrust
OS
exposed ridge
mesic slope
snow bed
wetland
d
i
w

Supplementary Figures (8.1-8.18)

Vascular plants on plots – Knudsenheia

* dominant species

K 1.1

- *Salix polaris*
- *Saxifraga oppositifolia* *
- *Luzula confusa*
- *Cerastium arcticum*

K 1.2

- *Salix polaris*
- *Saxifraga oppositifolia* *
- *Draba alpina*
- *Minuartia* sp.
- *Sagina nivalis*
- *Cerastium arcticum*
- *Arenaria* sp.

K 1.3

- *Silene acaulis* *
- *Saxifraga oppositifolia* *
- *Salix polaris*
- *Minuartia* sp.
- *Luzula confusa*
- *Pedicularis hirsuta*
- *Arenaria* sp.

K 2.1

- *Salix polaris* *
- *Luzula confusa*
- *Saxifraga oppositifolia*
- *Silene acaulis*
- *Minuartia* sp.
- *Bistorta vivipara*

K 2.2

- *Saxifraga oppositifolia* *
- *Salix polaris*
- *Luzula confusa*
- *Draba alpina*
- *Bistorta vivipara*
- *Oxyria digyna*
- *Saxifraga cespitosa*

K 2.3

- *Saxifraga oppositifolia* *
- *Salix polaris*
- *Draba alpina*
- *Bistorta vivipara*
- *Oxyria digyna*
- *Minuartia* sp.
- *Carex* sp.
- *Arenaria* sp.

K 3.1

- *Sagina nivalis*
- *Saxifraga oppositifolia* *
- *Oxyria digyna*
- *Saxifraga cespitosa*
- *Salix polaris*
- *Luzula nivalis*

K 3.2

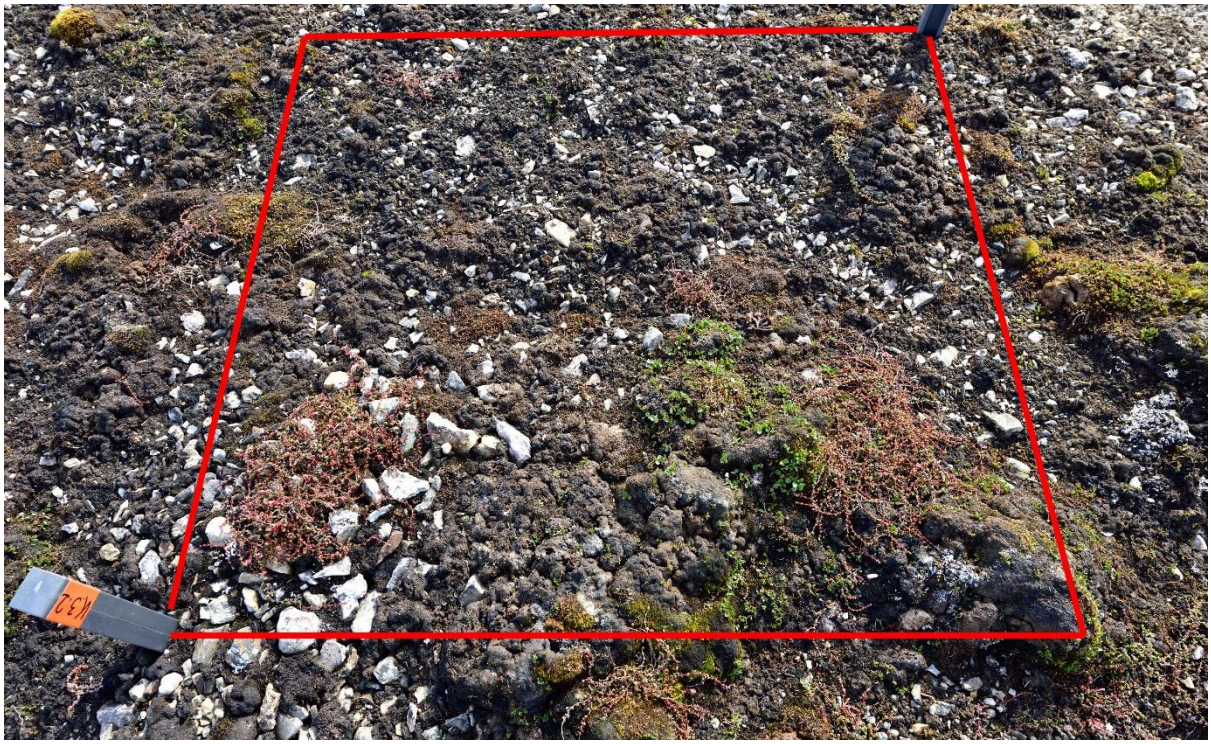

- *Saxifraga oppositifolia* *
- *Salix polaris*
- *Sagina nivalis*
- *Saxifraga cespitosa*
- *Arenaria* sp.
- *Poa* sp.

K 3.3

- *Saxifraga oppositifolia* *
- *Salix polaris*
- *Carex* sp.
- *Cardamine pratensis* ssp. *angustifolia*
- *Saxifraga cespitosa*
- *Sagina nivalis*
- *Arenaria* sp.

Vascular plants on plots – Ossian Sarsfjellet

* dominant species

<u>O 1.1</u>

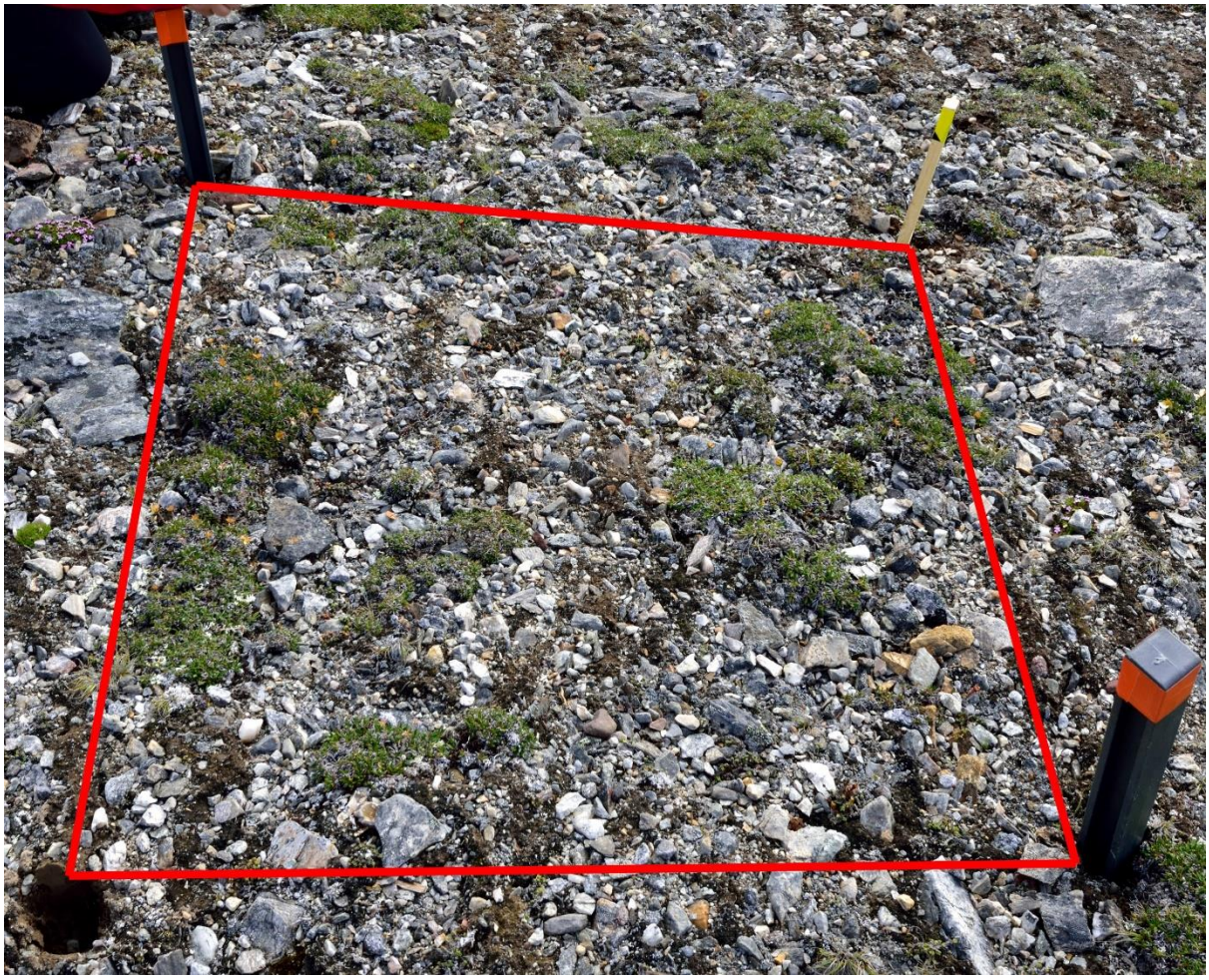

- *Dryas octopetala* *
- *Luzula nivalis*
- *Saxifraga oppositifolia*

O 1.2

- *Dryas octopetala* *
- *Luzula nivalis*
- *Saxifraga oppositifolia*
- *Silene acaulis*

O 1.3

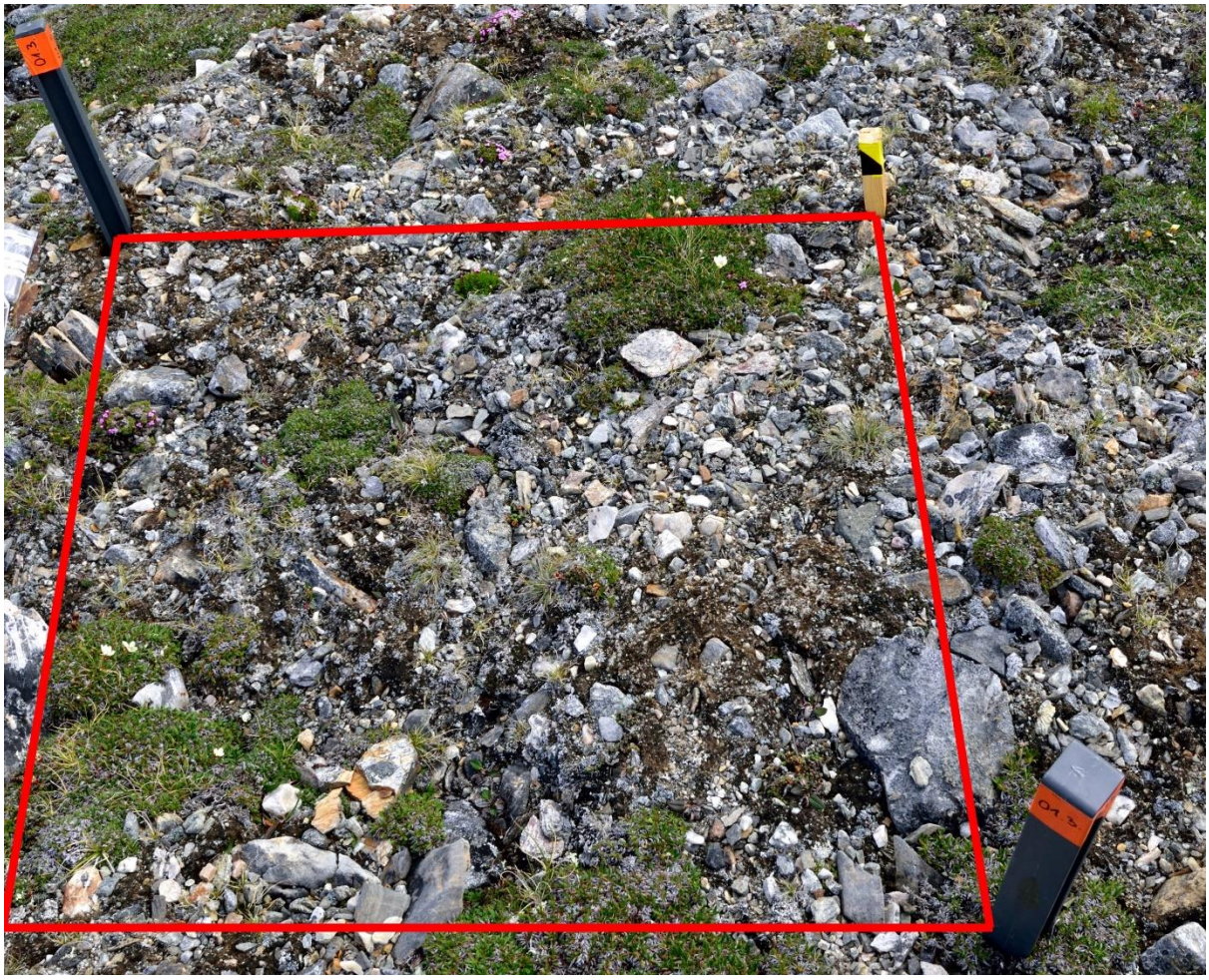

- *Dryas octopetala* *
- *Luzula nivalis* *
- *Silene acaulis*
- *Bistorta vivipara*
- *Saxifraga oppositifolia*

O 2.1

0 2.1

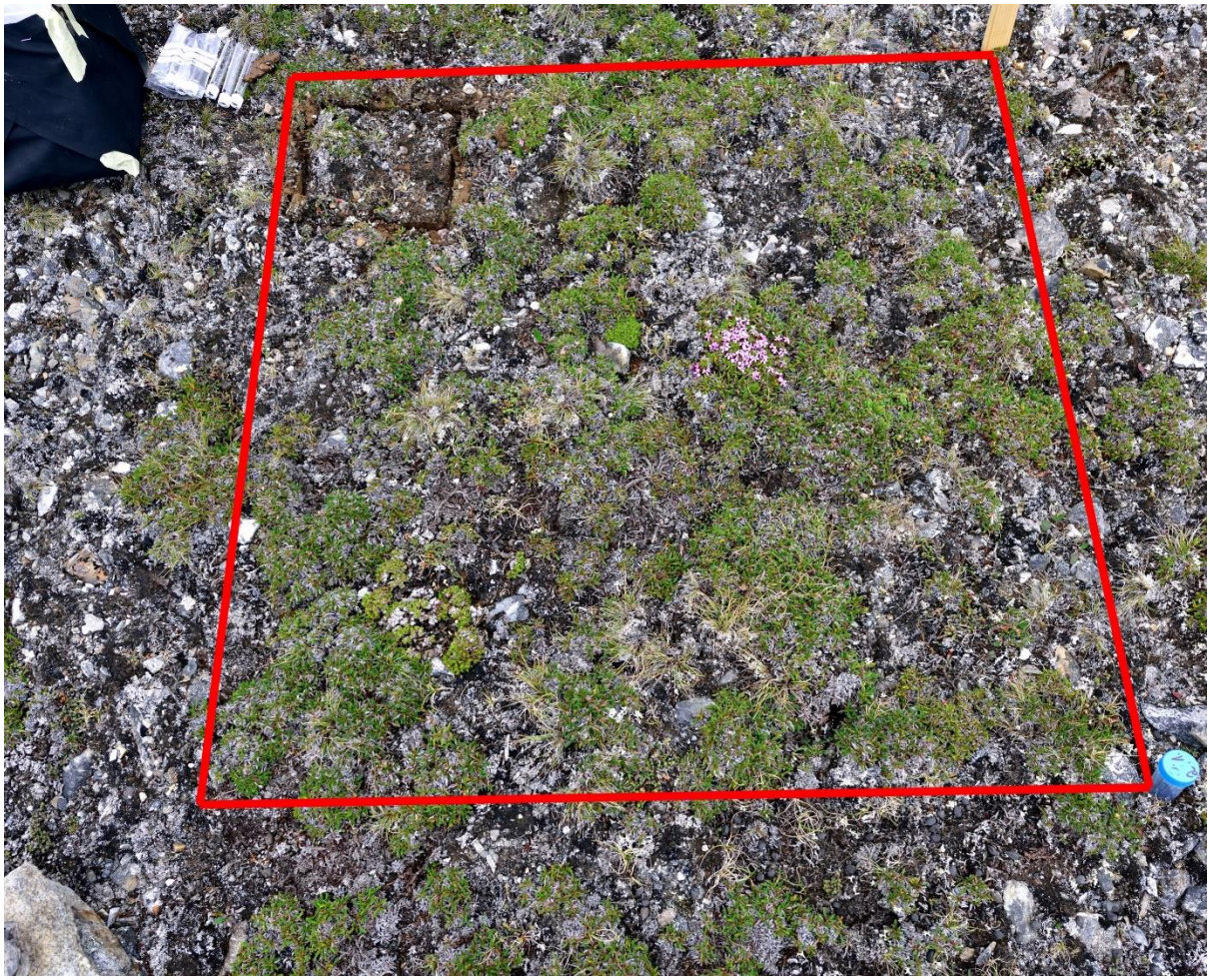

- *Silene acaulis*
- *Dryas octopetala* *
- *Bistorta vivipara*
- *Poa* sp.
- *Saxifraga oppositifolia*

O 2.2

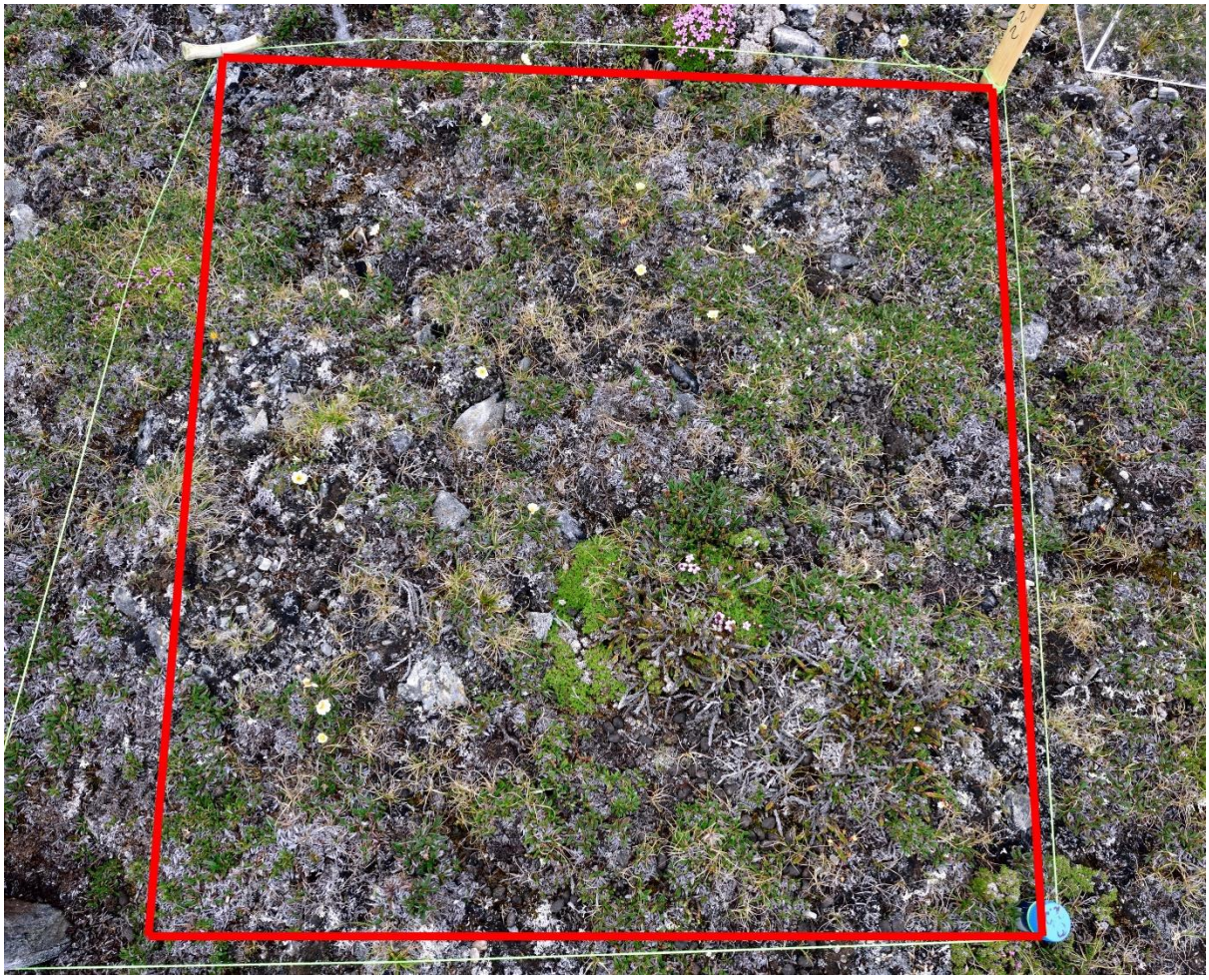

- *Silena acaulis*
- *Dryas octopetala*
- *Saxifraga oppositifolia*
- *Festuca* sp. *
- *Cassiopa tetragona*

O 2.3

- *Dryas octopetala* *
- *Saxifraga oppositifolia*
- *Luzula confua*
- *Poa* sp.
- *Festuca* sp.

O 3.1

- *Salix polaris* *
- *Saxifraga oppositifolia*

O 3.2

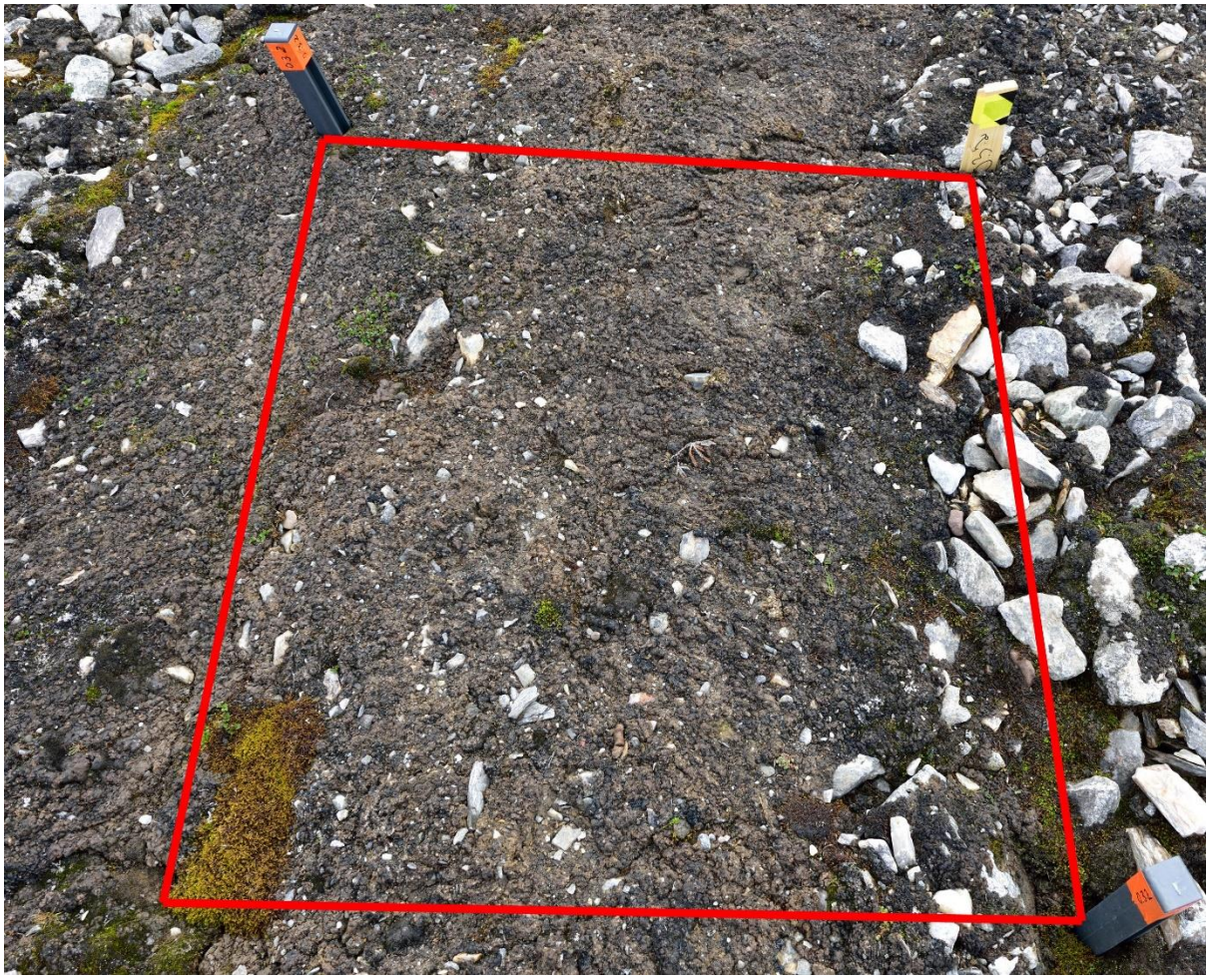

- *Salix polaris* *
- *Cardamine pratensis* ssp. *angustifolia*
- *Saxifraga oppositifolia*

O 3.3

- *Salix polaris*
- *Cassiope tetragona*
- *Saxifraga cernua*
- *Saxifraga oppositifolia*
- *Arenaria* sp.

Supplementary Figure 9